MDM2/MDM4 expression pattern implicates *TP53*-reactivation strategy for the treatment of *TP53*-wild-type cancers

（野生型 ***TP53*** 腫瘍治療において ***TP53*** 再活性化戦略の重要因子と考えられる **MDM2/MDM4** 発現パターン）

２０１４

筑波大学大学院博士課程人間総合科学研究科

廣　瀬　充　明

Abstract

MDM2 and MDM4, a structurally related MDM2 homolog, negatively regulates expression and functions of *TP53* tumor suppressor gene. To explore the precise expression patterns and function of *MDM2* and *MDM4* in wild-type (wt) *TP53* cancer cells, we analyzed 11 various cancer cell lines with wt *TP53*. All cell lines exhibited deregulated expression of MDM2 or MDM4, and were divided into two distinct types; the one expressing high levels of MDM4 and another expressing low levels of MDM4. The low MDM4 type expressed higher MDM2 levels than the high MDM4 type. In cells with high MDM4 expression, knockdown of *MDM4* or *MDM2* reactivated *TP53*, and simultaneous knockdown of *MDM2* and *MDM4* synergistically reactivated *TP53*. In contrast, in cells with low MDM4 expression, knockdown of only *MDM2* reactivated *TP53*. These results suggest that both *MDM2* and *MDM4* are closely involved in *TP53* inactivation in cancer cells with high MDM4 expression, whereas only *MDM2*, and not *MDM4*, is a regulator of *TP53* in cells with low MDM4 expression. MDM4 expression in wt *TP53*-tumors is a potential indicator for *TP53* reactivation cancer therapy by simultaneous targeting of *MDM4* and *MDM2*. Specific knockdown of *MDM2* and *MDM4* might be applicable for *TP53* restoration therapy.

Introduction

The tumor suppressor protein p53 is a transcriptional factor that controls multiple genes to regulate the cell cycle, apoptosis, DNA repair, and senescence [1-4]. Approximately half of human cancers have mutations in the *TP53* gene [5], indicating that *TP53* inactivation is pivotal in cancer development. The remaining cancers retain the wild-type (wt) status of *TP53*, which is inhibited by deregulated upstream modulators and/or inactivation of downstream effectors [1, 6].

The human homolog of murine double minute 2 (MDM2) is a major negative regulator of p53 through binding to its transactivation domain, thereby resulting in subsequent suppression of transcriptional activity [7, 8]. In addition, the RING (Really Interesting New Gene) finger domain of MDM2 functions as an E3 ubiquitin ligase that mediates ubiquitin-dependent degradation of p53 [9-11]. *MDM2* is a transcriptional target of p53, forming an autoregulatory feedback loop [12, 13]. *TP53* is also negatively regulated by MDM4, an MDM2 homologue [14, 15]. Like MDM2, MDM4 represses p53 transcriptional activity by direct binding of its binding domain, which is located in the N-terminal region, to the transactivation domain of p53 [14]. Although MDM4 possess a RING finger domain, it lacks E3 ligase activity and is unable to directly decrease p53 stability [14], but rather enhances the E3 ligase activity toward p53 by forming a heterodimer with MDM2 via the RING domains of both molecules [16, 17]. MDM2 also destabilizes the structure of MDM4 via ubiquitination [18]. Both *MDM2* and *MDM4* function as oncogenes and their deregulated expression has been reported in various types of human cancers, including soft tissue sarcoma, breast cancer, retinoblastoma, and melanoma [19-23]. However, to date, the expression patterns and functional roles of *MDM2* and *MDM4* in cancer cells with or without *TP53* mutations remain uncertain.

Restoration of wt *TP53* function in tumors leads to rapid tumor regression by induction of apoptosis or senescence and can be applicable to cancer treatment [19]. Several small molecular inhibitors of the interactions between MDM2 and p53 have been shown to restore *TP53* activity in tumors expressing high MDM2 levels [24-26]. Similarly, MDM4 antagonists have been reported. Among them, SAH-p53-8 binds and inhibits more efficiently to MDM4 than to MDM2 and exerts antitumor effects in cancer cells expressing high MDM4 levels [21, 27].

Synthetic small interfering RNAs (siRNAs) are not only a powerful tool for functional gene analysis [28, 29], but has been intensively explored for application to therapy of human cancer and other diseases with some promising results [30-32]. siRNAs often silence the expression of untargeted genes with partial sequence complementarities (off-target effects) [33, 34]. Base-paring between mRNA sequences and the seed regions of siRNA guide strands (nucleotide positions 2–8 from the 5′ end) may be sufficient for off-target silencing [33]. However, such nonspecific effects can be avoided by DNA replacement in the seed region of the guide strand (first 6–8 bases from the 5′ end) and the complementary sequences of the passenger strand, which has been designated as a double-stranded RNA–DNA chimera (dsRDC) [35]. Additionally, dsRDCs are more stable in the human serum than the conventional siRNA due to resistance to endogenous ribonuclease [36]. Considering the recent progress in RNAi technology, synthetic siRNAs targeting *MDM2* and *MDM4* may present an alternative mechanism to induce *TP53* restoration.

In the present study, we carefully analyzed MDM2 and MDM4 expression levels in various cancer cell lines with and without *TP53* mutations and found that MDM2 or MDM4 were deregulated in all wt *TP53* cancer cells. To probe the roles of *MDM2* and *MDM4* in *TP53* regulation in cancer cells, we selected efficient and specific dsRDC-modified siRNAs targeting *MDM2* and *MDM4*. Individual and combined knockdown of *MDM2* and *MDM4*

revealed their roles in *TP53* inactivation in wt *TP53* cancer cells with different patterns of MDM2 and MDM4 expression, which provided us with a rationale for the selection of *MDM2* and *MDM4* as targets in *TP53* restoration therapy of cancers.

Results

Expression levels of MDM2 and MDM4 in cancer cell lines

We examined the expression levels of MDM2 and MDM4 in 14 cancer cell lines including 11 wt *TP53* and three mutant (mt) *TP53* cell lines by immunoblotting (Figure 1). wt *TP53* cell lines were divided into two groups according to levels of MDM4: seven cell lines (MCF-7, A375, SNU-1, HCT116, NUGC-4, LoVo, and A549) expressed high levels of MDM4, whereas the remaining four cell lines (SJSA-1, HepG2, HuH-6, and C32TG) expressed low levels of MDM4. Interestingly, all cell lines expressing low MDM4 levels accumulated higher levels of MDM2 than those expressing high MDM4 levels. Cell lines carrying mt *TP53* (KATOIII, NUGC-3, and DLD-1) expressed various levels of MDM4 and MDM2. p53 was not detected in KATOIII cells, which harbored gross deletions of both *TP53* alleles.

Efficient siRNAs targeting MDM2 and their DNA-modified forms

Seventeen new siRNAs targeting human *MDM2* transcript variant 1 (NM_002392.4) were selected using siDirect software (Supplementary Table 1) [37]. These siRNAs contained at least three mismatched base pairs in both the guide and passenger strands with a non-redundant sequence set of human genes to minimize off-target effects [38]. siRNA sequences containing single-nucleotide polymorphisms were also excluded to avoid individual differences in response. These new siRNAs targeting *MDM2* (siMDM2) and nine previously

reported siMDM2s were synthesized and tested for knockdown efficiency by transfection into SJSA-1 cells and subsequent immunoblot analysis (Figure 2a) (Supplementary Figure 1). Six new (1068, 830, 480, 691, 1489, and 2381) and two previously reported siMDM2s (396 and 851) strongly suppressed MDM2 expression. These siMDM2s were converted to dsRDCs with the aim to further reduce off-target effects by decreasing the free energy of pairing stability between the seed region and off-target mRNAs [35]. As shown in Figure 2b, all dsRDC-modified siMDM2s (chiMDM2) were able to silence MDM2 expression with the most efficient silencing achieved by chiMDM2-1489. Quantitative reverse transcription (qRT)-PCR analysis demonstrated the ability of these chiMDM2s to knockdown mRNA to the same or a slightly reduced extent as compared with cognate siRNAs (Supplementary Figure 2).

The effect of chiMDM2s on the growth of cancer cells with high MDM2 expression was examined. SJSA-1 cells were transfected with chiMDM2s at 1 nM for 5 days and then subjected to the WST-8 (2-(2-methoxy-4-nitrophenyl)-3-(4-nitrophenyl)-5-(2,4-disulfophenyl)-2H-tetrazolium) cell proliferation assay. As shown in Figure 2c, most of the chiMDM2s suppressed the growth of SJSA-1 cells in proportion to the individual *MDM2* knockdown efficiency, with the exception of chiMDM2-1068, which suppressed cell growth to a greater extent than chiMDM2-1489, although the *MDM2* knockdown efficiency was inversed, suggesting that chiMDM2-1068 partially exerted MDM2–p53-indepndent growth suppression. Therefore, these two chiMDM2s were further analyzed for growth suppression of cancer cells carrying mt *TP53* (KATO III, NUGC-3, and DLD-1) (Figure 2d). chiMDM2-1489 and chiMDM2-1068 exhibited negligible effects on these cells, with the exception of chiMDM2-1068-mediated suppression of NUGC-3 cell growth.

Selection of siRNAs targeting MDM4 and their DNA-modified forms

siRNAs targeting the coding region of human *MDM4* transcript variant 1 (NM_002393.4) were similarly selected as those targeting *MDM2*. Ten new *MDM4* siRNAs (siMDM4) (Supplementary Table 1) were examined for *MDM4* knockdown efficiency in MCF-7 cells, which exhibit high levels of MDM4 expression, by immunoblot analysis (Figure 3a). Seven siMDM4s (317, 347, 452, 582, 788, 861, and 1036) showed strong suppression of MDM4 expression and were converted to dsRDCs (chiMDM4). Six chiMDM4s (317, 347, 452, 788, 861, and 1036) knocked down MDM4 expression in MCF-7 cells as efficiently as their cognate siRNAs (Figure 3b). Among these six chiMDM4s, chiMDM4-452 exhibited the highest silencing activity. qRT-PCR analysis confirmed efficient *MDM4* knockdown by each of these chiMDM4s (Supplementary Figure 3). The effect on viability of MCF-7 cells by these chiMDM4s was also tested using the WST-8 assay (Figure 3c). All chiMDM4s induced growth suppression in parallel to the *MDM4* knockdown efficiency of each. In fact, potent growth suppression was observed with most chiMDM4s (317, 347, 452, 788, 861, and 1036). chiMDM4-582 exhibited less efficient *MDM4* silencing and growth inhibitory activities of MCF-7 cells than other chiMDM4s.

Next, the effect of each chiMDM4 on the growth of mt *TP53* cancer cells was evaluated. Six effective chiMDM4s were introduced into three mt *TP53* cancer cell lines (KATO III, NUGC-3, and DLD-1) and examined for effects on cell growth suppression using the WST-8 assay. As shown in Figure 3d, chiMDM4-452 and -1036 showed negligible growth suppression, whereas other chiMDM4s exhibited mild growth suppression, but without any statistical differences.

Effects of MDM4 and MDM2 knockdown on growth of wt TP53 cancer cells

To examine the effect of *MDM4* and *MDM2* knockdown on the growth of wt *TP53* cancer cells, we tested the 11 previously mentioned wt *TP53* cancer cell lines, which included seven with high levels of MDM4 expression (MCF-7, A375, SNU-1, HCT116, NUGC-4, LoVo, and A549) and four with low levels of MDM4 expression (SJSA-1, HepG2, HuH-6, and C32TG). To knock down *MDM2* and *MDM4*, two dsRDCs were chosen for each target (chiMDM2-1068/-1489 and chiMDM4-452/-1036). As shown in Figure 4, each chiMDM2 inhibited growth of all wt *TP53* cancer cells regardless of the expression levels of MDM2 or MDM4, whereas chiMDM4 only suppressed the growth of cells with high MDM4 expression and not of those with low MDM4 expression (Figure 4).

Next, we examined the effects of *MDM2* and *MDM4* knockdown on expression levels of p53 and $p21^{Waf1/Cip1}$ (p21), a *TP53* responsive gene product [39], by immunoblotting. As shown in Figure 5, *MDM2* suppression increased levels of p53 and p21 in all wt *TP53* cells. MDM4 slightly accumulated in most of the wt *TP53* cells after *MDM2* knockdown, with the exception of SJSA-1 and HepG2 cells. As shown in Figure 6, in all cells with high MDM4 expression, *MDM4* knockdown slightly increased p53 levels in association with the induction of p21 and MDM2, which are known *TP53*-responsive genes, but had negligible effects on p53, p21, and MDM2 in cells with low MDM4 expression.

The effects of *MDM2* and *MDM4* knockdown on p53 and MDM4 varied among three mt *TP53* cell lines. As shown in Figures 5, *MDM2* knockdown induced mild MDM4 accumulation in NUGC-3 and DLD-1 cells, but not KATOIII cells. As shown in Figure 6, *MDM4* knockdown reduced MDM2 levels in all three mt *TP53* cell lines. Accumulation of p53 occurred in DLD-1 cells, which expressed low levels of mt p53, but not in NUGC-3 cells, which expressed high levels of mt p53. The induction of p21 did not occur in any of these mt *TP53* cell lines in response to *MDM2* or *MDM4* knockdown.

Effects of MDM2/MDM4 double knockdown on growth of wt TP53 cancer cells

We examined the effect of *MDM2*/*MDM4* double knockdown on growth of wt *TP53* cells, which had high MDM4 expression, using chiMDM4-452 and chiMDM2-1489, which were the most potent and specific inhibitors of each respective target. Cells were transfected with various chiMDM4 concentrations along with control dsRDC-modified siRNA (chiCtrl) at a total dosage of 2 nM, as indicated. As shown in Figure 7a, chiMDM4 and chiMDM2 suppressed the growth of MCF-7 and A375 cells in a dose-dependent manner. When chiMDM2 and chiMDM4 were simultaneously transfected at three different ratios, more profound growth suppression was observed in these cells than transfection of either chiMDM2 or chiMDM4 alone at the same dosage, or even at a maximal dosage of 2 nM. Similar enhancement in growth suppression was observed in all cells with high MDM4 expression, including five other cell lines (SNU-1, HCT116, NUGC-4, LoVo, and A549) (Supplementary Figure 4). Combination index values at three different ratios of chiMDM2 and chiMDM4 were calculated in cells with high MDM4 expression with values ranging between 0.20 and 0.72, which showed that these dsRDCs promoted synergistic growth inhibition of tumor cells with high MDM4 expression (Table 1).

chiMDM2, but not chiMDM4, alone dose-dependently suppressed the growth of cells with low MDM4 expression (SJSA-1 and C32TG). Further, chiMDM2-mediated growth inhibition was not enhanced by co-transfection with chiMDM4 in these cells (Figure 7a). Similar results were observed in two other cell lines with low MDM4 expression (Supplementary Figure 5). In mt *TP53* cells, chiMDM2, chiMDM4, and a combination of both failed to demonstrate any detectable growth suppression (Supplementary Figure 5).

Effect of MDM2/MDM4 double knockdown on p53 expression

To explore the mechanism by which *MDM2*/*MDM4* double knockdown synergistically inhibited the growth of cells with high MDM4 expression, the effects of individual and simultaneous knockdown of *MDM2* and *MDM4* on p53 expression was examined in MCF-7 and A375 cells (Figure 7b). *MDM2* knockdown was associated with mild accumulation of MDM4 and p53, as well as the product of the downstream gene *p21*. *MDM4* knockdown slightly increased levels of MDM2 and p21 in these cells. A subtle increase in p53 expression was observed in chiMDM4-transfected A375 cells, but not in chiMDM4-transfected MCF-7 cells. Simultaneous knockdown by chiMDM2 (1 nM) and chiMDM4 (1 nM) induced expression of p53 and the downstream *p21* gene product more than either chiMDM2 or chiMDM4 alone at 1 or 2 nM in cell lines with high MDM4 expression (MCF-7, A375). In cells with low MDM4 expression (SJSA-1 and C32TG), chiMDM2 alone knocked down MDM2, which resulted in accumulation of both p53 and p21 (Figure 7b). However, chiMDM4 did not induce either p53 or p21 upregulation even though MDM4 was efficiently suppressed. Co-transfection of chiMDM2 and chiMDM4 induced accumulation of p53 and p21 to the same extent as chiMDM2.

Discussion

A fraction of wt *TP53* tumors expresses oncogenes, such as *MDM2* and *MDM4*, to inactivate *TP53* [19]. Precise expression patterns and the functional significance of *MDM2* and *MDM4* in wt *TP53* cancer cells remain to be clarified. In the present study, a careful analysis of cancer cell lines harboring wt and mt *TP53* demonstrated that all wt *TP53* cancer cell lines included in this study exhibited deregulated expression of MDM2 or MDM4. These cell lines were divided into just two distinct types, according to MDM4 expression levels; the one

expressing MDM4 at high levels and another expressing MDM4 at low levels. MDM4 expression occurs when tumor cells have acquired *MDM4* amplification [19], activated *KRAS* mutations [40], or loss of miR-34a-mediated suppression [41]. Among seven wt *TP53* cancer cell lines with high MDM4 expression, one cell line (MCF-7) has MDM4 amplification [42]. Four cell lines (SNU-1, HCT116, LoVo, A549) harbor *KRAS* mutation [43, 44], suggesting that the deregulated expression of MDM4 may be caused by *KRAS* activation or along with miR-34a abnormality in these cell lines.

It is well established that *MDM2* and *MDM4* are ideal therapeutic targets for wt *TP53* tumors. However, to date, there is no biological rationale of whether *MDM2* or *MDM4* should be targeted in such tumors. Using wt *TP53* cell lines and DNA-modified siRNAs specific to *MDM2* and *MDM4*, we demonstrated here for the first time that knockdown of either *MDM4* or *MDM2* alone can reactivate the *TP53* pathway in cancer cells with high MDM4 expression, whereas knockdown of *MDM2*, but not *MDM4*, can reactivate wt *TP53* in the low *MDM4* cancer cells. Furthermore, simultaneous knockdown of *MDM2* and *MDM4* synergistically activated *TP53* and suppressed cell growth in the cancer cells with high MDM4 expression. Based on these results, we propose that both *MDM4* and *MDM2* are efficient therapeutic targets in wt *TP53* tumors cells with high MDM4 expression, whereas *MDM2*, but not necessarily *MDM4*, presents a possible therapeutic target in wt *TP53* cancer cells with low MDM4 expression.

We explored the mechanisms by which *MDM2*/*MDM4* double knockdown exhibited synergistic effects on *TP53* activation in tumor cells with high MDM4 expression. MDM4 is devoid of a nuclear transport signal and requires MDM2 to translocate from the cytoplasm to nucleus [45, 46]. Therefore, we assessed whether the synergistic effect of *MDM2*/*MDM4* double knockdown on *TP53* activation was mediated through the inhibition of nuclear transport of MDM4 by MDM2 (Supplementary Figure 6). We found that *MDM2* knockdown

had no effect on nuclear localization of MDM4 in cells with high MDM4 expression (A375), suggesting that this nuclear localization was independent of MDM2 expression in these cells and that synergistic activation of *TP53* was not mediated by inhibition of nuclear transport of MDM4 in these cells. In cells with high MDM4 expression, *MDM4* silencing alone increased p53 expression. Because MDM4 has no intrinsic ubiquitin ligase function, but can enhance MDM2 ubiquitin ligase activity by forming a heterodimer with MDM2 [14, 17], both MDM2 and MDM4 may be involved in p53 degradation through the formation of heterodimers. Alternatively, *MDM4* knockdown alone enhances *MDM2* expression by releasing p53 transcriptional activity, which subsequently suppresses p53 [12, 14, 47]. Therefore, simultaneous knockdown of *MDM4* and *MDM2* may result in more potent activation of p53 by blocking this p53-MDM2 negative feedback than silencing MDM4 alone.

With the aim to employ synthetic siRNAs in *TP53*-restoration therapy, we carefully designed and screened siRNAs with high specificities and potencies to target either *MDM2* or *MDM4*. A series of siRNAs targeting *MDM2* and *MDM4* was designed using siDirect software, which enabled the selection of siRNA sequences with structural features compatible for the efficient loading of the guide strand into the RNA-induced silencing complex as well as a minimal number of off-target candidates from human genes [37, 48]. Among them, effective siRNAs with high knockdown efficiency were chosen by cell-transfection experiments and then converted to DNA-modified siRNAs with 6-base pair double-stranded DNA substitutions [35]. This modification offers a great advantage by lowering off-target activity by decreasing the free energy between the seed regions and off-target mRNAs and avoiding passenger strand-mediated RNAi [35, 49]. Three dsRDCs targeting *MDM2* (chiMDM2-1489, 1068, and 2381) and six targeting *MDM4* (chiMDM4-861, 452, 1036, 317, 347, and 788) showed potent silencing activity at a concentration as low as 1 nM. siRNAs interfere with the endogenous miRNA pathway by competing with molecules involved in

miRNA production, such as AGO2, when introduced at high concentrations [50-52]. Intracellular concentrations of most functional miRNAs are between 3 and 100 nM [53]. To avoid disruptions to the miRNA pathway, it is necessary to introduce siRNAs with high silencing activities into cells at the lowest concentrations possible. dsRDCs targeting *MDM2* and *MDM4* selected in this study had a half maximal inhibitory concentration (IC_{50} value) of less than 1 nM and were used at 1 nM in most of our experiments. With the development of an efficient delivery system of oligonucleotides, dsRDCs targeting *MDM2* and *MDM4* could be applied to the treatment of wt *TP53* cancers.

Some earlier reports using *TP53* switchable mice with *MDM2*- and *MDM4*-deficient backgrounds showed transient restoration of *TP53* activity in normal tissues in the absence of *MDM2*, resulting in 100% fatality within 5–6 days [54], whereas *TP53* activation in the absence of *MDM4* was nonlethal and reversible [55]. These data indicate that systemic administration of MDM4 inhibitors may be better tolerated than MDM2 inhibitors, therefore, *MDM4* knockdown using our dsRDC might be a valuable therapeutic strategy for treatment of tumors with high MDM4 expression levels but no *TP53* mutations. Currently, we are exploring expression patterns of MDM2, MDM4, and p53 as well as the genotypes of various human tumor samples.

Some cancer cells expressing high levels of MDM4 are reportedly resistant to small-molecule MDM2 inhibitors [56-58]. However, our results clearly demonstrated that specific *MDM2* knockdown suppressed growth of wt *TP53* cells regardless of the expression levels of MDM2 and MDM4. The action mechanisms of small molecular inhibitors and siRNAs differ because small molecular inhibitors bind MDM2 at the p53-binding pocket and disrupt MDM2–p53 interactions and increase p53 expression, resulting in enhanced *MDM2* induction, which might dysregulate other *MDM2*-target molecules. In contrast, siRNAs targeting *MDM2* suppress only *MDM2*. This phenomenon might explain the discrepancy in our results.

Besides controlling *TP53* activity, MDM2 has been reported to regulate E2F1 transcriptional activity and expression of p21, FOXO3a, and XIAP [59-62]. MDM4 has been also reported to inhibit p21 and Smad family proteins [63, 64]. The results of the present study showed that knockdown of *MDM2* and *MDM4* by respective dsRDCs at 1 nM had no effect on growth of mt *TP53* cancer cells expressing various levels of MDM4, suggesting that growth suppression by *MDM2* and *MDM4* knockdown is entirely dependent on wt *TP53* and that suppression of *TP53*-independent activities had a minimal effect on vitro growth of tumors expressing mt *TP53*. The mild growth suppression of NUGC-3 and DLD-1 cells observed by transfection of chiMDM2-1489 at 2 nM suggested the presence of nonspecific effects, such as inhibition of miRNA generation, even though the siRNA concentration was very low.

In conclusion, we showed that most wt *TP53* cancer cells exhibited deregulation of MDM2 and MDM4. Specific knockdown of *MDM2* and *MDM4* with DNA-modified siRNAs clearly revealed the ability of *MDM2* and *MDM4* to inactivate wt *TP53* in cancer cells. The results of this study provide rationale for the selection of *MDM2* and *MDM4* as therapeutic targets in cancer cells expressing wt *TP53*. MDM4 expression in wt *TP53*-tumors is a potential indicator for *TP53* reactivation by combined *MDM4* and *MDM2*-targeted cancer therapy. Our specific and potent DNA-modified siRNAs targeting *MDM2* and *MDM4* might be applicable to *TP53* restoration therapy for human cancers.

Materials and methods

Cell lines

Fourteen tumor cell lines were used: eleven cell lines with wt *TP53* (MCF-7 breast cancer, A375 melanoma, HCT116 colon cancer, NUGC-4 gastric cancer, LoVo colon cancer, SJSA-1

osteosarcoma, HepG2 hepatocellular carcinoma, HuH-6 hepatocellular carcinoma, A549 lung cancer, and C32TG melanoma) [43, 65-67], and three cell lines with mt *TP53* (KATOIII gastric cancer, NUGC-3 gastric cancer, and DLD-1 colon cancer) [65]. The MCF-7, A375, SNU-1, HCT116, LoVo, SJSA-1, and DLD-1 cell lines were purchased from the American Type Culture Collection (Rockville, MD, USA). The NUGC-4, HepG2, and KATOIII cell lines were obtained from the Riken BioResource Center Cell Bank (Tsukuba, Japan). The NUGC-3, A549, HuH-6 and C32TG cell lines were obtained from the Japanese Collection of Research Bioresources Cell Bank (Osaka, Japan). MCF-7, SNU-1, NUGC-4, SJSA-1, KATOIII, NUGC-3, and DLD-1 cells were cultured in RPMI 1640 medium (Sigma–Aldrich, St. Louis, MO, USA) supplemented with 10% fetal bovine serum (FBS; Nichirei Biosciences, Tokyo, Japan). A375, HepG2, and HuH-6 cells were cultured in Dulbecco's modified Eagle's medium (Sigma–Aldrich) containing 10% FBS. HCT116 cells were cultured in McCoy's 5A medium (Sigma–Aldrich) with 10% FBS. LoVo cells were cultured in Ham's F12K medium (Invitrogen, Carlsbad, CA, USA) with 10% FBS.

siRNAs and transfection

Sequences of siRNAs used in this study are summarized in Supplementary Table 1. All siRNAs targeting *MDM2* and *MDM4* were designed using siDirect software (http://sidirect2.rnai.jp), as reported previously [37]. The control siRNA was an artificial sequence designed to have all features of siRNAs inducing potent RNAi and the least homology to human and mouse genes. Control-R siRNA consisted of randomized sequences of the control siRNA. Control siRNA and complementary dsRDC-modified forms were included in all experiments. siRNAs were converted to dsRDCs by substituting six ribonucleotides from the 5′ end of the guide strand and eight from the 3′ end of the passenger

strand with corresponding deoxynucleotides [35, 68]. siRNA transfection was performed using Lipofectamine RNAiMAX (Invitrogen) as reported previously [68].

Immunoblot analysis

Sodium dodecyl sulfate-polyacrylamide gel electrophoresis and immunoblot analysis were performed as previously described [69]. The primary and secondary antibodies used in this study were as follows: mouse monoclonal antibody against MDM2 (2A10) (Abcam, Cambridge, UK); rabbit polyclonal antibody against MDM4 (Bethyl Laboratories, Montogomery, TX, USA); mouse monoclonal antibodies against $p21^{Waf1/Cip1}$ (DCS60) and β-actin (8H10D10) (Cell Signaling Technology, Danvers, MA, USA); and anti-TP53 mouse monoclonal antibody (BP53-12; Cell Sciences, Canton, MA, USA). Both horseradish peroxidase-conjugated anti-mouse IgG sheep and anti-rabbit IgG donkey sera were purchased from GE Healthcare (Buckinghamshire, UK). Chemiluminescent detection was performed using ECL Prime Western Blotting Detection Reagent (GE Healthare) and the Ez-Capture II Imaging System (Atto Corp., Tokyo, Japan).

Quantitative reverse transcription (qRT)-PCR

RNA samples were extracted from cell lysate using 40 µL per well of RealTime ready Cell Lysis reagent (Roche Diagnostics, Mannheim, Germany), according to the manufacturer's instructions. cDNA was synthesized using 2 µL of RNA and Transcriptor Universal cDNA Master (Roche Diagnostics) in 20 µL-reactions. qRT-PCR assays were performed using Applied Biosystems 7500 Fast Real-Time PCR System (Applied Biosystems, Foster City, CA, USA) in 96-well plates. Primers and TaqMan probes for *MDM2*, *MDM4*, and *18S ribosomal RNA* (*18SrRNA*) were obtained from Applied Biosystems (Assay ID: Hs00234753, Hs00967238, and Hs03928990_g1, respectively). Reactions were performed in duplicate

under standard thermocycling conditions in a 20-µL volume containing 0.8 µL of cDNA, 900 nM of primers, 250 nM of the probe, and 10 µL of TaqMan Gene Expression Master Mix (Applied Biosystems), according to the manufacturer's protocol. The amount of target mRNA was examined and normalized to that of *18S rRNA.*

Cell viability

WST-8 colorimetric assays were performed using a Cell Counting kit-8 (Dojin Laboratories, Kumamoto, Japan) according to the manufacturer's protocol. Cells were incubated for 5 days after transfection and then analyzed using an iMark microplate reader (Bio-Rad, Hercules, CA, USA). The absorbance of the plates was read at wavelengths of 450 nm and 620 nm.

Combination index.

Quantification of chiMDM2 and chiMDM4 synergy was determined by the Chou–Talalay method for drug combination using CalcuSyn software (Biosoft, Cambridge, UK) [70]. A combination index (CI) < 0.9 indicates synergism, 09–1.1 indicates additivity, and >1.1 indicates antagonism.

Immunofluorescence

Cells were fixed for 15 min in 4% paraformaldehyde at room temperature, and aldehydes were neutralized by soaking coverslips in phosphate-buffered saline (PBS) with 0.1% tween 20 (PBS-T) containing 50 mM glycine at room temperature. Then, the cells were permeabilized in PBS-T with 0.1% Triton X-100 solution for 15 min on ice, blocked for 60 min in PBS-T solution containing 5% normal goat serum (Vector Laboratories, Burlingame,

CA, USA) (blocking solution) at room temperature, and then reacted with rabbit polyclonal antibody against MDM4 (Bethyl Laboratories) diluted with blocking solution. After overnight incubation at 4°C, the cells were reacted with fluorescein isothiocyanate-conjugated goat anti-rabbit IgG antibody (Bethyl Laboratories) diluted with washing buffer for 60 min at room temperature. Nuclei were counterstained with 4′,6-diamidino-2-phenylindole (DAPI). Confocal fluorescence images were obtained using Leica TCS SP5 confocal microscope (Leica Microsystems GmbH, Wetzlar, Germany)

Statistical analysis.

All data are expressed as the mean ± standard deviation (SD). Statistical significance of differences between various groups was evaluated using the Dunnett's test. P-values < 0.05 were considered significant.

Acknowledgement

We thank Ms. M. Shinozaki for her technical assistance and Ms. J. Yamaguchi and Ms. M. Aida for their secretarial work. This work was supported in part by a Grant-in-Aid for Scientific Research (C) from the Ministry of Education, Culture, Sports, Science and Technology of Japan to H.I. (grant number: 26460624). We would like to thank Enago for the English language review.

References

1. Vogelstein B, Lane D, Levine AJ. Surfing the p53 network. Nature. 2000; 408: 307-310.

2. Vousden KH, Lu X. Live or let die: the cell's response to p53. Nat Rev Cancer. 2002; 2: 594-604.

3. Fridman JS, Lowe SW. Control of apoptosis by p53. Oncogene. 2003; 22: 9030-9040.

4. Pei D, Zhang Y, Zheng J. Regulation of p53: a collaboration between Mdm2 and Mdmx. Oncotarget. 2012; 3: 228-35.

5. Hainaut P, Hernandez T, Robinson A, Rodriguez-Tome P, Flores T, Hollstein M, Harris CC, Montesano R. IARC Database of p53 gene mutations in human tumors and cell lines: updated compilation, revised formats and new visualisation tools. Nucleic Acids Res. 1998; 26: 205-13.

6. Toledo F, Wahl GM. Regulating the p53 pathway: in vitro hypotheses, in vivo veritas. Nat Rev Cancer. 2006; 6: 909-923.

7. Momand J, Zambetti GP, Olson DC, George D, Levine AJ. The mdm-2 oncogene product forms a complex with the p53 protein and inhibits p53-mediated transactivation. Cell. 1992; 69: 1237-1245.

8. Oliner JD, Pietenpol JA, Thiagalingam S, Gyuris J, Kinzler KW, Vogelstein B. Oncoprotein MDM2 conceals the activation domain of tumour suppressor p53. Nature. 1993; 362: 857-860.

9. Haupt Y, Maya R, Kazaz A, Oren M. Mdm2 promotes the rapid degradation of p53. Nature. 1997; 387: 296-299.

10. Kubbutat MH, Jones SN, Vousden KH. Regulation of p53 stability by Mdm2. Nature. 1997; 387: 299-303.

11. Demidenko ZN, Blagosklonny MV. Flavopiridol induces p53 via initial inhibition of Mdm2 and p21 and, independently of p53, sensitizes apoptosis-reluctant cells to tumor necrosis factor. Cancer Res. 2004; 64: 3653-3660.

12. Piette J, Neel H, Marechal V. Mdm2: keeping p53 under control. Oncogene. 1997; 15: 1001-1010.

13. Pant V, Lozano G. Dissecting the p53-Mdm2 feedback loop in vivo: uncoupling the role in p53 stability and activity. Oncotarget. 2014; 5: 1149-1156.

14. Shvarts A, Steegenga WT, Riteco N, van Laar T, Dekker P, Bazuine M, van Ham RC, van der Houven van Oordt W, Hateboer G, van der Eb AJ, Jochemsen AG. MDMX: a

novel p53-binding protein with some functional properties of MDM2. EMBO J. 1996; 15: 5349-5357.

15. Tan BX, Khoo KH, Lim TM, Lane DP. High Mdm4 levels suppress p53 activity and enhance its half-life in acute myeloid leukaemia. Oncotarget. 2014; 5: 933-943.

16. Tanimura S, Ohtsuka S, Mitsui K, Shirouzu K, Yoshimura A, Ohtsubo M. MDM2 interacts with MDMX through their RING finger domains. FEBS Lett. 1999; 447: 5-9.

17. Linares LK, Hengstermann A, Ciechanover A, Muller S, Scheffner M. HdmX stimulates Hdm2-mediated ubiquitination and degradation of p53. Proc Natl Acad Sci U S A. 2003; 100: 12009-12014.

18. Pan Y, Chen J. MDM2 promotes ubiquitination and degradation of MDMX. Mol Cell Biol. 2003; 23: 5113-21.

19. Wade M, Li YC, Wahl GM. MDM2, MDMX and p53 in oncogenesis and cancer therapy. Nat Rev Cancer. 2013; 13: 83-96.

20. Laurie NA, Donovan SL, Shih C-S, Zhang J, Mills N, Fuller C, Teunisse A, Lam S, Ramos Y, Mohan A, Johnson D, Wilson M, Rodriguez-Galindo C et al. Inactivation of the p53 pathway in retinoblastoma. Nature. 2006; 444: 61-66.

21. Gembarska A, Luciani F, Fedele C, Russell EA, Dewaele M, Villar S, Zwolinska A, Haupt S, de Lange J, Yip D, Goydos J, Haigh JJ, Haupt Y et al. MDM4 is a key therapeutic target in cutaneous melanoma. Nat Med. 2012; 18: 1239-1247.

22. Ramos YF, Stad R, Attema J, Peltenburg LT, van der Eb AJ, Jochemsen AG. Aberrant expression of HDMX proteins in tumor cells correlates with wild-type p53. Cancer Res. 2001; 61: 1839-1842.

23. Wang YV, Wade M, Wong E, Li YC, Rodewald LW, Wahl GM. Quantitative analyses reveal the importance of regulated Hdmx degradation for p53 activation. Proc Natl Acad Sci U S A. 2007; 104: 12365-12370.

24. Vassilev LT. In Vivo Activation of the p53 Pathway by Small-Molecule Antagonists of MDM2. Science. 2004; 303: 844-848.

25. Shangary S, Qin D, McEachern D, Liu M, Miller RS, Qiu S, Nikolovska-Coleska Z, Ding K, Wang G, Chen J, Bernard D, Zhang J, Lu Y et al. Temporal activation of p53 by a specific MDM2 inhibitor is selectively toxic to tumors and leads to complete tumor growth inhibition. Proc Natl Acad Sci U S A. 2008; 105: 3933-3938.

26. Endo S, Yamato K, Hirai S, Moriwaki T, Fukuda K, Suzuki H, Abei M, Nakagawa I, Hyodo I. Potent in vitro and in vivo antitumor effects of MDM2 inhibitor nutlin-3 in gastric cancer cells. Cancer Sci. 2011; 102: 605-613.

27. Bernal F, Wade M, Godes M, Davis TN, Whitehead DG, Kung AL, Wahl GM, Walensky LD. A stapled p53 helix overcomes HDMX-mediated suppression of p53. Cancer Cell. 2010; 18: 411-422.

28. Elbashir SM, Harborth J, Lendeckel W, Yalcin A, Weber K, Tuschl T. Duplexes of 21-nucleotide RNAs mediate RNA interference in cultured mammalian cells. Nature. 2001; 411: 494-498.

29. Caplen NJ, Parrish S, Imani F, Fire A, Morgan RA. Specific inhibition of gene expression by small double-stranded RNAs in invertebrate and vertebrate systems. Proc Natl Acad Sci U S A. 2001; 98: 9742-9747.

30. Tabernero J, Shapiro GI, LoRusso PM, Cervantes A, Schwartz GK, Weiss GJ, Paz-Ares L, Cho DC, Infante JR, Alsina M, Gounder MM, Falzone R, Harrop J et al. First-in-humans trial of an RNA interference therapeutic targeting VEGF and KSP in cancer patients with liver involvement. Cancer Discov. 2013; 3: 406-417.

31. Fitzgerald K, Frank-Kamenetsky M, Shulga-Morskaya S, Liebow A, Bettencourt BR, Sutherland JE, Hutabarat RM, Clausen VA, Karsten V, Cehelsky J, Nochur SV, Kotelianski V, Horton J et al. Effect of an RNA interference drug on the synthesis of proprotein convertase subtilisin/kexin type 9 (PCSK9) and the concentration of serum LDL cholesterol in healthy volunteers: a randomised, single-blind, placebo-controlled, phase 1 trial. Lancet. 2014; 383: 60-68.

32. Coelho T, Adams D, Silva A, Lozeron P, Hawkins PN, Mant T, Perez J, Chiesa J, Warrington S, Tranter E, Munisamy M, Falzone R, Harrop J et al. Safety and efficacy of RNAi therapy for transthyretin amyloidosis. N Engl J Med. 2013; 369: 819-829.

33. Jackson AL, Bartz SR, Schelter J, Kobayashi SV, Burchard J, Mao M, Li B, Cavet G, Linsley PS. Expression profiling reveals off-target gene regulation by RNAi. Nat Biotechnol. 2003; 21: 635-637.

34. Saxena S, Jonsson ZO, Dutta A. Small RNAs with imperfect match to endogenous mRNA repress translation. Implications for off-target activity of small inhibitory RNA in mammalian cells. J Biol Chem. 2003; 278: 44312-44319.

35. Ui-Tei K, Naito Y, Zenno S, Nishi K, Yamato K, Takahashi F, Juni A, Saigo K. Functional dissection of siRNA sequence by systematic DNA substitution: modified siRNA with a DNA seed arm is a powerful tool for mammalian gene silencing with significantly reduced off-target effect. Nucleic Acids Res. 2008; 36: 2136-2151.

36. Kawata E, Ashihara E, Nakagawa Y, Kiuchi T, Ogura M, Yao H, Sakai K, Tanaka R, Nagao R, Yokota A, Takeuchi M, Kimura S, Hirai H et al. A combination of a DNA-chimera siRNA against PLK-1 and zoledronic acid suppresses the growth of malignant mesothelioma cells in vitro. Cancer Lett. 2010; 294: 245-53.

37. Naito Y, Yamada T, Ui-Tei K, Morishita S, Saigo K. siDirect: highly effective, target-specific siRNA design software for mammalian RNA interference. Nucleic Acids Res. 2004; 32: W124-W129.

38. Yamada T, Morishita S. Accelerated off-target search algorithm for siRNA. Bioinformatics. 2005; 21: 1316-24.

39. Sherr CJ, Roberts JM. CDK inhibitors: positive and negative regulators of G1-phase progression. Genes Dev. 1999; 13: 1501-1512.

40. Gilkes DM, Pan Y, Coppola D, Yeatman T, Reuther GW, Chen J. Regulation of MDMX expression by mitogenic signaling. Mol Cell Biol. 2008; 28: 1999-2010.

41. Okada N, Lin CP, Ribeiro MC, Biton A, Lai G, He X, Bu P, Vogel H, Jablons DM, Keller AC, Wilkinson JE, He B, Speed TP et al. A positive feedback between p53 and miR-34 miRNAs mediates tumor suppression. Genes Dev. 2014; 28: 438-450.

42. Danovi D, Meulmeester E, Pasini D, Migliorini D, Capra M, Frenk R, de Graaf P, Francoz S, Gasparini P, Gobbi A, Helin K, Pelicci PG, Jochemsen AG et al. Amplification of Mdmx (or Mdm4) directly contributes to tumor formation by inhibiting p53 tumor suppressor activity. Mol Cell Biol. 2004; 24: 5835-5843.

43. Forbes SA, Bindal N, Bamford S, Cole C, Kok CY, Beare D, Jia M, Shepherd R, Leung K, Menzies A, Teague JW, Campbell PJ, Stratton MR et al. COSMIC: mining complete cancer genomes in the Catalogue of Somatic Mutations in Cancer. Nucleic Acids Res. 2011; 39: D945-D950.

44. Yoon YK, Kim HP, Han SW, Hur HS, Oh do Y, Im SA, Bang YJ, Kim TY. Combination of EGFR and MEK1/2 inhibitor shows synergistic effects by suppressing EGFR/HER3-dependent AKT activation in human gastric cancer cells. Mol Cancer Ther. 2009; 8: 2526-2536.

45. Migliorini D. Hdmx Recruitment into the Nucleus by Hdm2 Is Essential for Its Ability to Regulate p53 Stability and Transactivation. J Biol Chem. 2001; 277: 7318-7323.

46. Gu J. Mutual Dependence of MDM2 and MDMX in Their Functional Inactivation of p53. J Biol Chem. 2002; 277: 19251-19254.

47. Wade M, Wang YV, Wahl GM. The p53 orchestra: Mdm2 and Mdmx set the tone. Trends Cell Biol. 2010; 20: 299-309.

48. Ui-Tei K, Naito Y, Takahashi F, Haraguchi T, Ohki-Hamazaki H, Juni A, Ueda R, Saigo K. Guidelines for the selection of highly effective siRNA sequences for mammalian and chick RNA interference. Nucleic Acids Res. 2004; 32: 936-948.

49. Ui-Tei K, Naito Y, Nishi K, Juni A, Saigo K. Thermodynamic stability and Watson-Crick base pairing in the seed duplex are major determinants of the efficiency of the siRNA-based off-target effect. Nucleic Acids Res. 2008; 36: 7100-7109.

50. Castanotto D, Sakurai K, Lingeman R, Li H, Shively L, Aagaard L, Soifer H, Gatignol A, Riggs A, Rossi JJ. Combinatorial delivery of small interfering RNAs reduces RNAi efficacy by selective incorporation into RISC. Nucleic Acids Research. 2007; 35: 5154-5164.

51. Grimm D, Streetz KL, Jopling CL, Storm TA, Pandey K, Davis CR, Marion P, Salazar F, Kay MA. Fatality in mice due to oversaturation of cellular microRNA/short hairpin RNA pathways. Nature. 2006; 441: 537-541.

52. Khan AA, Betel D, Miller ML, Sander C, Leslie CS, Marks DS. Transfection of small RNAs globally perturbs gene regulation by endogenous microRNAs. Nature Biotechnol. 2009; 27: 549-555.

53. Chen C, Ridzon DA, Broomer AJ, Zhou Z, Lee DH, Nguyen JT, Barbisin M, Xu NL, Mahuvakar VR, Andersen MR, Lao KQ, Livak KJ, Guegler KJ. Real-time quantification of microRNAs by stem-loop RT-PCR. Nucleic Acids Res. 2005; 33: e179.

54. Ringshausen I, O'Shea CC, Finch AJ, Swigart LB, Evan GI. Mdm2 is critically and continuously required to suppress lethal p53 activity in vivo. Cancer Cell. 2006; 10: 501-514.

55. Garcia D, Warr MR, Martins CP, Brown Swigart L, Passegue E, Evan GI. Validation of MdmX as a therapeutic target for reactivating p53 in tumors. Genes Dev. 2011; 25: 1746-1757.

56. Hu B, Gilkes DM, Farooqi B, Sebti SM, Chen J. MDMX Overexpression Prevents p53 Activation by the MDM2 Inhibitor Nutlin. J Biol Chem. 2006; 281: 33030-33035.

57. Patton JT. Levels of HdmX Expression Dictate the Sensitivity of Normal and Transformed Cells to Nutlin-3. Cancer Res. 2006; 66: 3169-3176.

58. Wade M, Wong ET, Tang M, Stommel JM, Wahl GM. Hdmx Modulates the Outcome of P53 Activation in Human Tumor Cells. J Biol Chem. 2006; 281: 33036-33044.

59. Martin K, Trouche D, Hagemeier C, Sorensen TS, La Thangue NB, Kouzarides T. Stimulation of E2F1/DP1 transcriptional activity by MDM2 oncoprotein. Nature. 1995; 375: 691-694.

60. Jin Y, Lee H, Zeng SX, Dai MS, Lu H. MDM2 promotes p21waf1/cip1 proteasomal turnover independently of ubiquitylation. EMBO J. 2003; 22: 6365-77.

61. Yang JY, Zong CS, Xia W, Yamaguchi H, Ding Q, Xie X, Lang JY, Lai CC, Chang CJ, Huang WC, Huang H, Kuo HP, Lee DF et al. ERK promotes tumorigenesis by inhibiting FOXO3a via MDM2-mediated degradation. Nat Cell Biol. 2008; 10: 138-148.

62. Gu L, Zhu N, Zhang H, Durden DL, Feng Y, Zhou M. Regulation of XIAP translation and induction by MDM2 following irradiation. Cancer Cell. 2009; 15: 363-375.

63. Jin Y, Zeng SX, Sun XX, Lee H, Blattner C, Xiao Z, Lu H. MDMX promotes proteasomal turnover of p21 at G1 and early S phases independently of, but in cooperation with, MDM2. Mol Cell Biol. 2008; 28: 1218-1229.

64. Kadakia M, Brown TL, McGorry MM, Berberich SJ. MdmX inhibits Smad transactivation. Oncogene. 2002; 21: 8776-8785.

65. Jia LQ, Osada M, Ishioka C, Gamo M, Ikawa S, Suzuki T, Shimodaira H, Niitani T, Kudo T, Akiyama M, Kimura N, Matsuo M, Mizusawa H et al. Screening the p53 status of human cell lines using a yeast functional assay. Mol Carcinog. 1997; 19: 243-253.

66. Bressac B, Galvin KM, Liang TJ, Isselbacher KJ, Wands JR, Ozturk M. Abnormal structure and expression of p53 gene in human hepatocellular carcinoma. Proc Natl Acad Sci U S A. 1990; 87: 1973-1977.

67. Phelps RM, Johnson BE, Ihde DC, Gazdar AF, Carbone DP, McClintock PR, Linnoila RI, Matthews MJ, Bunn PA, Jr., Carney D, Minna JD, Mulshine JL. NCI-Navy Medical Oncology Branch cell line data base. J Cell Biochem Suppl. 1996; 24: 32-91.

68. Yamato K, Egawa N, Endo S, Ui-Tei K, Yamada T, Saigo K, Hyodo I, Kiyono T, Nakagawa I. Enhanced specificity of HPV16 E6E7 siRNA by RNA–DNA chimera modification. Cancer Gene Ther. 2011; 18: 587-597.

69. Ueno T, Endo S, Saito R, Hirose M, Hirai S, Suzuki H, Yamato K, Hyodo I. The Sirtuin Inhibitor Tenovin-6 Upregulates Death Receptor 5 and Enhances Cytotoxic

Effects of 5-Fluorouracil and Oxaliplatin in Colon Cancer Cells. Oncol Res. 2014; 21: 155-164.

70. Chou TC, Talalay P. Quantitative analysis of dose-effect relationships: the combined effects of multiple drugs or enzyme inhibitors. Adv Enzyme Regul. 1984; 22: 27-55.

Figure Legends

Figure 1. Expression levels of p53, MDM2, and MDM4 in cancer cell lines.

Expression levels of p53, MDM2, and MDM4 were examined in 14 cancer cell lines (11 wt *TP53* cell lines and 3 mt *TP53* cell lines) by immunoblotting. SE, short exposure; LE, long exposure.

Figure 2. Effects of siRNAs targeting *MDM2* and their dsRDC forms on MDM2 expression and cell growth. (a) Two previously reported (396 and 851) and 17 new siMDM2s were analyzed for their effects on MDM2 expression in SJSA-1 cells by immunoblotting. SJSA-1 cells were transfected with mock, control siRNA (siCtrl), control-R siRNA (siCtrl-R), and siMDM2s at 1 nM for 48 h and then examined for MDM2 expression by immunoblotting. (b) Control siRNA, control-R siRNA, and eight effective siMDM2s, including two previously reported and six new were converted to dsRDC forms (chiCtrl, chiCtrl-R, and chiMDM2s), and examined for MDM2 knockdown activity in SJSA-1 cells 48 h after transfection at 1 nM. (c) Effect of chiMDM2s on growth of SJSA-1 cells were examined. The cells were transfected with control dsRDC (chiCtrl) or eight chiMDM2s at 1 nM for 5 days and then assayed for relative viable cell number using the WST-8 assay (mean ± SD; n = 3). (d) The

effects of two highly effective chiMDM2s (1068 and 1489) on growth of mt *TP53*-cancer cells (KATOIII, NUCG-3, and DLD-1) after transfection at 1 nM for 5 days were examined using theWST-8 assay. Viable cell numbers relative to those transfected with control dsRDC (chiCtrl) are shown (mean ± SD; n = 3; *$p < 0.05$; Dunnett's test).

Figure 3. Effects of siRNAs targeting *MDM4* and their dsRDC forms on MDM4 expression and cell growth. (a) The effects of siMDM4s on MDM4 expression were analyzed in MCF-7 cells by immunoblotting 48 h after transfection with mock, control siRNA (siCtrl), or 10 siMDM4s at 1 nM. SE, short exposure; LE, long exposure. (b) Seven effective siMDM4s and a control siRNA were converted to dsRDC forms (chiMDM4s and chiCtrl), and analyzed for MDM4 knockdown in MCF-7 cells 48 h after transfection at 1 nM. (c) The effect of chiMDM4s on the growth of MCF-7 cells was examined. The cells were transfected with control dsRDC (chiCtrl) or seven chiMDM4s at 1 nM for 5 days and then assayed for relative viable cell number using the WST-8 assay (mean ± SD; n = 3). (d) The effects of six highly effective chiMDM4s on the growth of mt *TP53*-cancer cells (KATOIII, NUCG-3, and DLD-1) after transfecting at 1 nM for 5 days were examined using the WST-8 assay. Viable cell numbers relative to those transfected with control dsRDC (chiCtrl) are shown (mean ± SD.; n = 3; *$p < 0.05$; Dunnett's test).

Figure 4. Effect of *MDM2* and *MDM4* knockdown on the growth of wt *TP53* cell lines. dsRDCs targeting *MDM2* (chiMDM2-1068 and chiMDM2-1489) (a), *MDM4* (chiMDM4-452 and chiMDM4-1036) (b) and control dsRDC (chiCtrl) were transfected into seven cell lines with high MDM4 expression levels (MCF-7, A375, SNU-1, HCT116, NUCG-4, LoVo, and A549) and four cell lines with low MDM4 expression levels (SJSA-1, HepG2, HuH-6,

and C32TG) at 1 nM. Five days after transfection, cell viability was determined using the WST-8 assay. Viable cell numbers relative to those transfected with chiCtrl are shown (mean ± SD; n = 3; *$p < 0.05$; Dunnett's test).

Figure 5. Effect of *MDM2* knockdown on expression levels of MDM2, MDM4, p53 and p21. Mock, control dsRDC (Ctrl), and two dsRDCs targeting *MDM2* (chiMDM2-1068, chiMDM2-1489) were transfected into seven cells lines with high MDM4 expression, four cell lines with low MDM4 expression and three mt *TP53* cell lines at 1 nM. Expression levels of MDM2, MDM4, p53, and p21 were analyzed by immunoblotting 2 days after transfection.

Figure 6. Effect of *MDM4* knockdown on expression levels of MDM4, MDM2, p53, and p21. Mock, control dsRDC (Ctrl), and two dsRDCs targeting *MDM4* (chiMDM4-452 and -1036) were transfected into seven cell lines with high MDM4 expression, four cell lines with low MDM4 expression and three mt *TP53* cell lines at 1 nM. Expression levels of MDM2, MDM4, p53, and p21 were analyzed by immunoblotting 2 days after transfection.

Figure 7. Combined knockdown of *MDM2* and *MDM4* in wt *TP53* cell lines with high and low MDM4 expression. Effects of individual and simultaneous knockdown of *MDM2* and *MDM4* on cell growth (a) and expression of p53 and p21 (b) were examined in two cell lines with high MDM4 expression (MCF-7 and A375) and two cell lines with low MDM4 expression (SJSA-1 and C32TG). Cells were transfected with *MDM4* dsRDC (chiMDM4-452) alone, *MDM2* dsRDC (chiMDM2-1489) alone, or both. The total amount of dsRDCs was adjusted to 2 nM by adding control dsRDC (chiCtrl). Cell viability was determined 5 days after transfection using the WST-8 assay. Viable cell numbers of chiCtrl (2 nM)

transfected cells was defined as 100% (mean ± SD; n = 3). Levels of MDM2, MDM4, p53, and p21 were analyzed by immunoblotting 2 days after transfection. In panel b, + and ++ indicates 1 nM and 2 nM of dsRDCs, respectively.

Figure 1

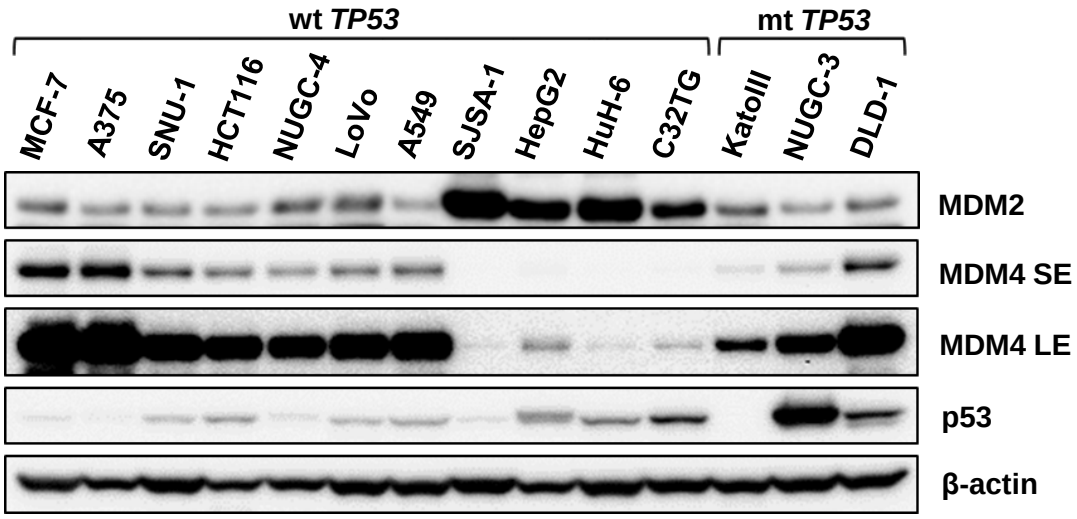
wt TP53
mt TP53
MCF-7
A375
SNU-1
HCT116
NUGC-4
LoVo
A549
SJSA-1
HepG2
HuH-6
C32TG
KatoIII
NUGC-3
DLD-1
MDM2
MDM4 SE
MDM4 LE
p53
β-actin

Figure 2

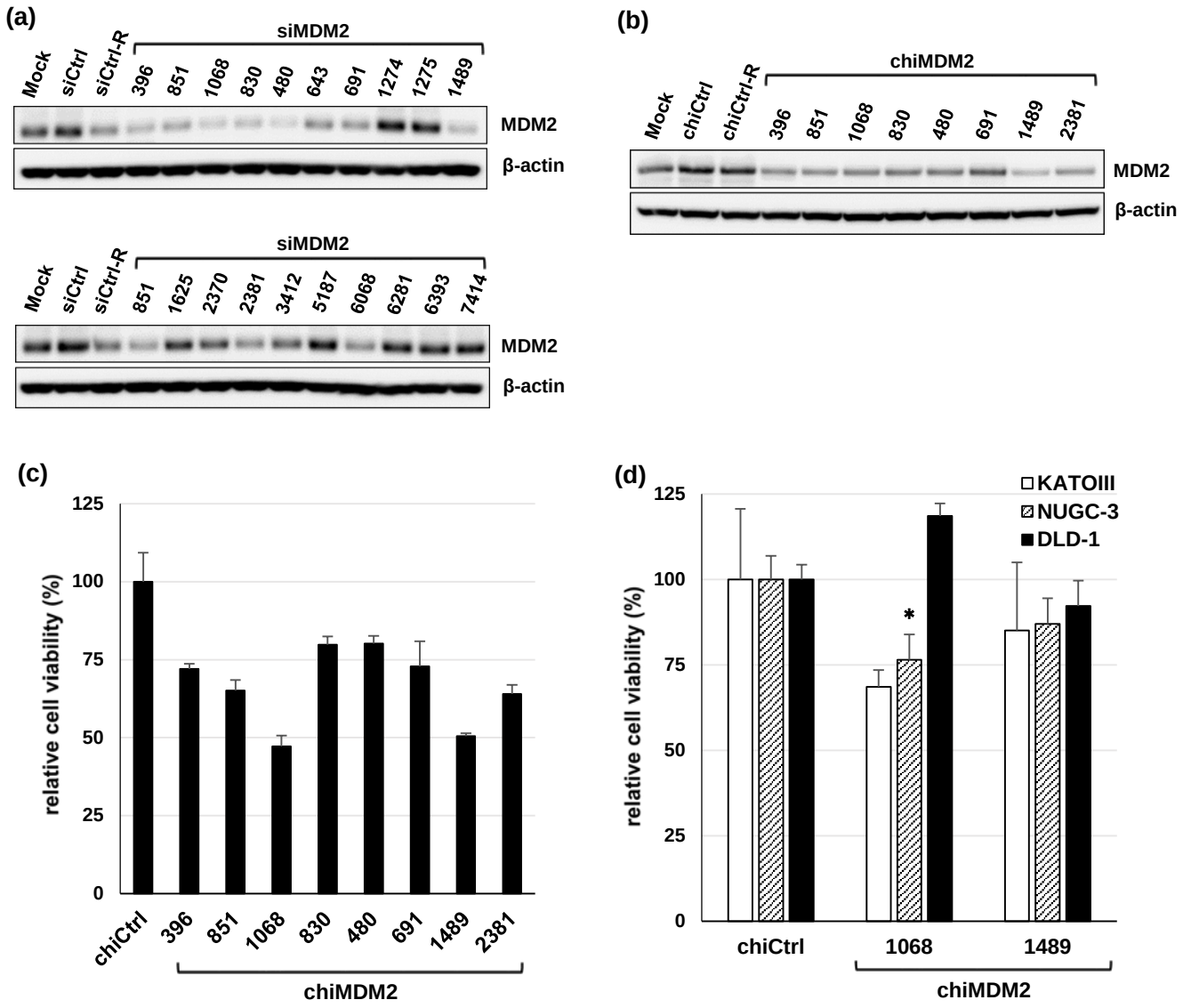
(a)
siMDM2
Mock
siCtrl
siCtrl-R
396
851
1068
830
480
643
691
1274
1275
1489
MDM2
β-actin
siMDM2
Mock
siCtrl
siCtrl-R
851
1625
2370
2381
3412
5187
6068
6281
6393
7414
MDM2
β-actin
(b)
chiMDM2
Mock
chiCtrl
chiCtrl-R
396
851
1068
830
480
691
1489
2381
MDM2
β-actin
(c)
relative cell viability (%)
125
100
75
50
25
0
chiCtrl
396
851
1068
830
480
691
1489
2381
chiMDM2
(d)
KATOIII
NUGC-3
DLD-1
relative cell viability (%)
125
100
75
50
25
0
*
chiCtrl
1068
1489
chiMDM2

Figure 3

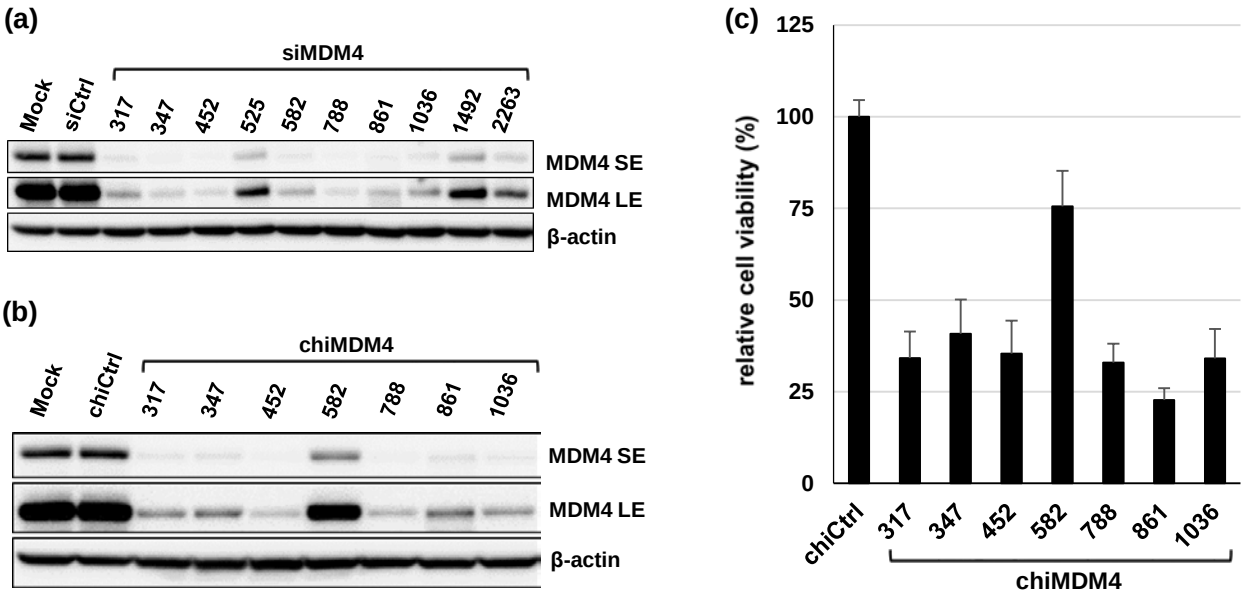
(a)
siMDM4
Mock
siCtrl
317
347
452
525
582
788
861
1036
1492
2263
MDM4 SE
MDM4 LE
β-actin
(b)
chiMDM4
Mock
chiCtrl
317
347
452
582
788
861
1036
MDM4 SE
MDM4 LE
β-actin
(c)
relative cell viability (%)
125
100
75
50
25
0
chiCtrl
317
347
452
582
788
861
1036
chiMDM4

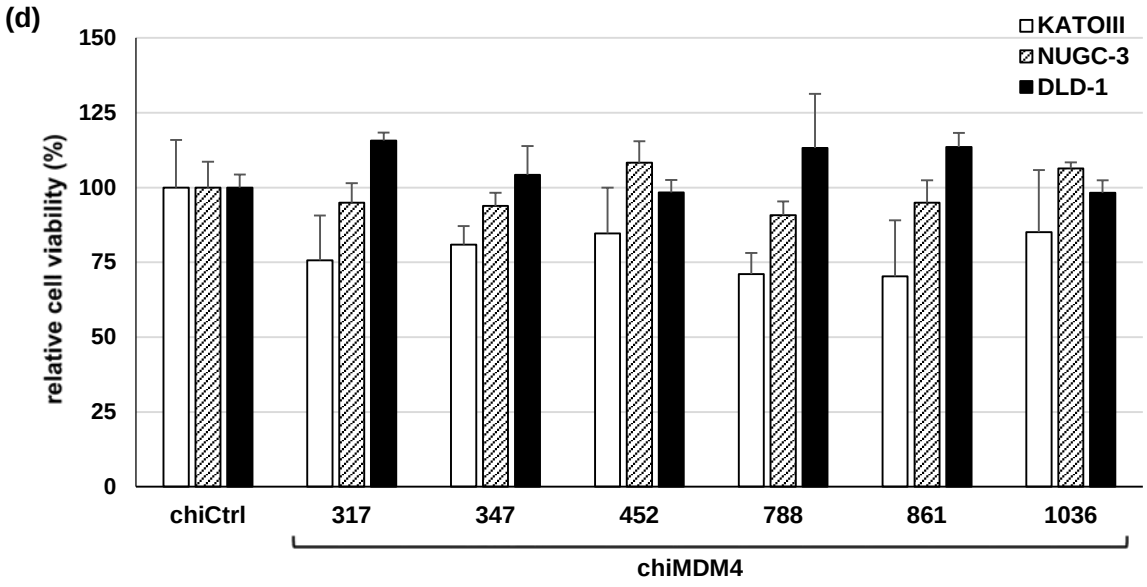
(d)
KATOIII
NUGC-3
DLD-1
relative cell viability (%)
150
125
100
75
50
25
0
chiCtrl
317
347
452
788
861
1036
chiMDM4

Figure 4

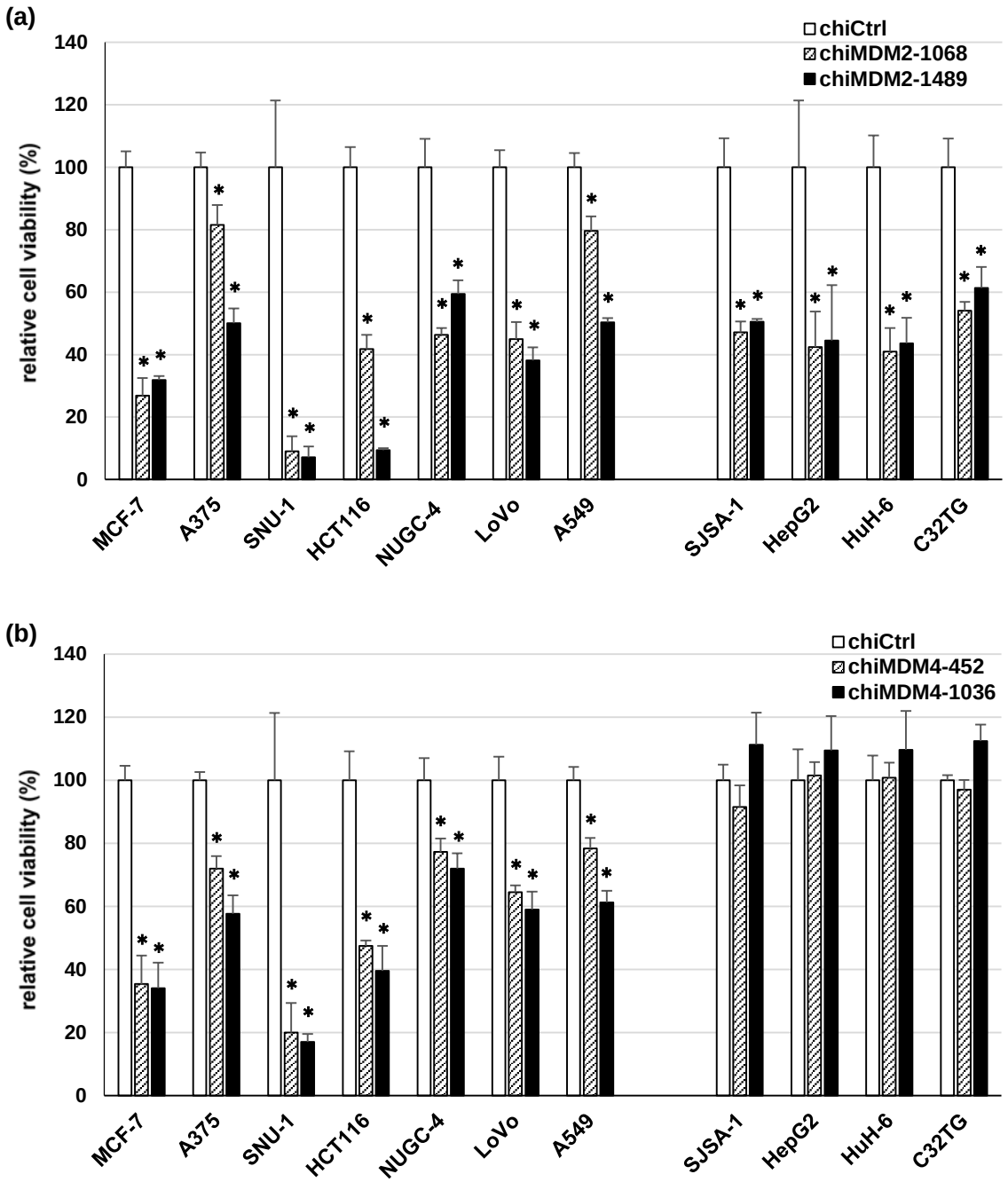
(a)
chiCtrl
chiMDM2-1068
chiMDM2-1489
relative cell viability (%)
0
20
40
60
80
100
120
140
MCF-7
A375
SNU-1
HCT116
NUGC-4
LoVo
A549
SJSA-1
HepG2
HuH-6
C32TG
(b)
chiCtrl
chiMDM4-452
chiMDM4-1036
relative cell viability (%)
0
20
40
60
80
100
120
140
MCF-7
A375
SNU-1
HCT116
NUGC-4
LoVo
A549
SJSA-1
HepG2
HuH-6
C32TG

Figure 5

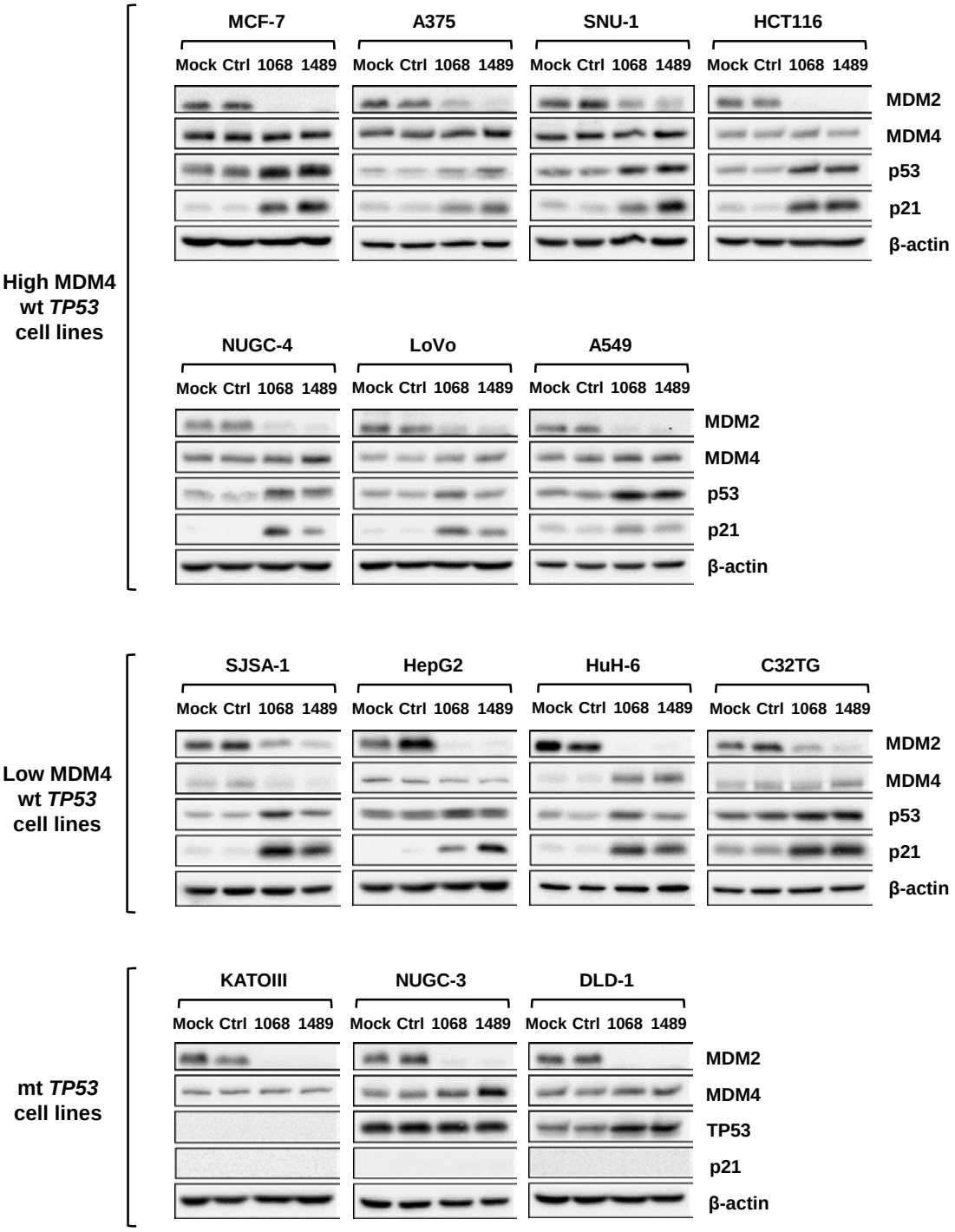
High MDM4
wt TP53
cell lines
MCF-7
A375
SNU-1
HCT116
Mock Ctrl 1068 1489
MDM2
MDM4
p53
p21
β-actin
NUGC-4
LoVo
A549
Low MDM4
wt TP53
cell lines
SJSA-1
HepG2
HuH-6
C32TG
mt TP53
cell lines
KATOIII
NUGC-3
DLD-1
TP53

Figure 6

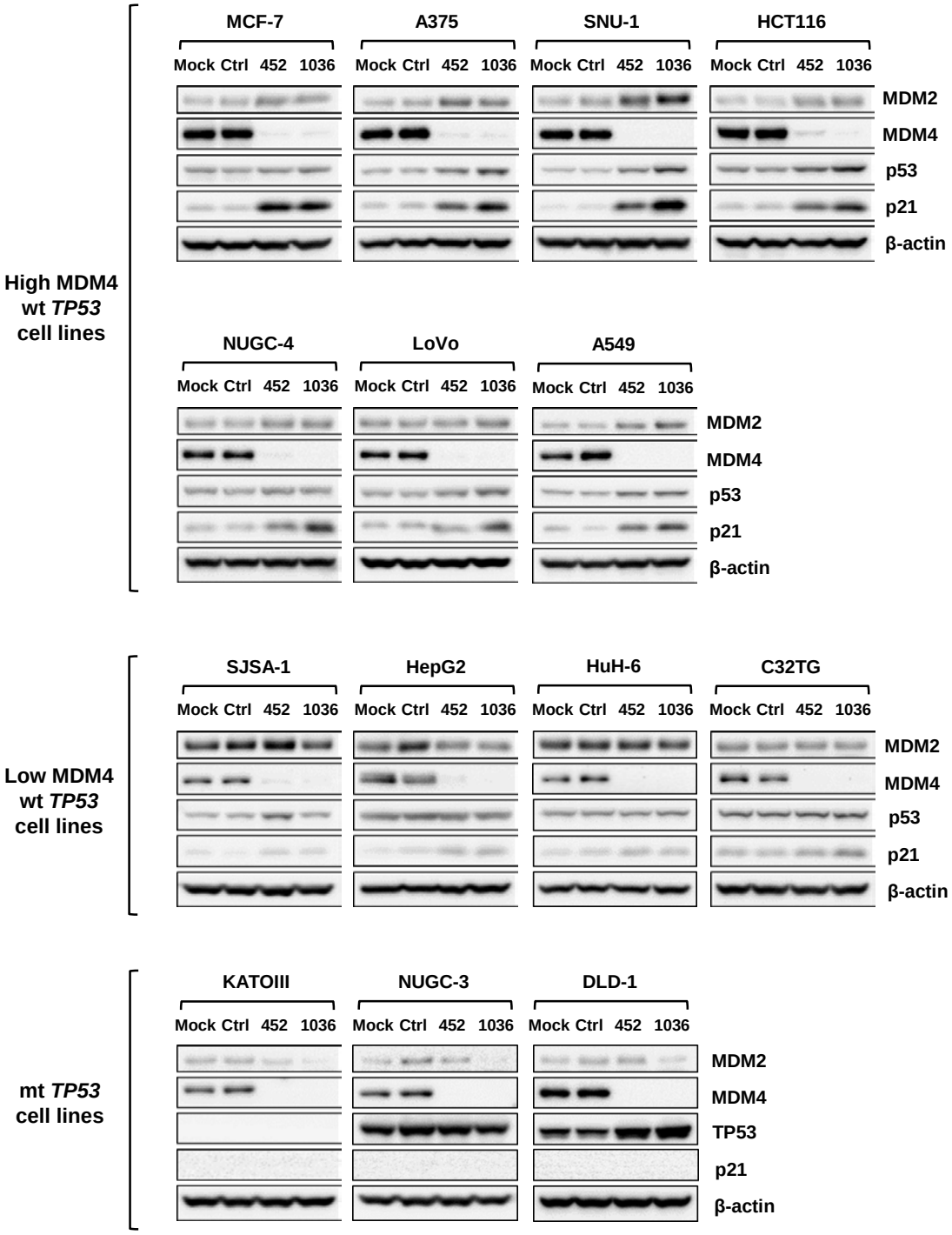
High MDM4
wt TP53
cell lines
MCF-7
A375
SNU-1
HCT116
Mock Ctrl 452 1036
MDM2
MDM4
p53
p21
β-actin
NUGC-4
LoVo
A549
Low MDM4
wt TP53
cell lines
SJSA-1
HepG2
HuH-6
C32TG
mt TP53
cell lines
KATOIII
NUGC-3
DLD-1
TP53

Figure 7

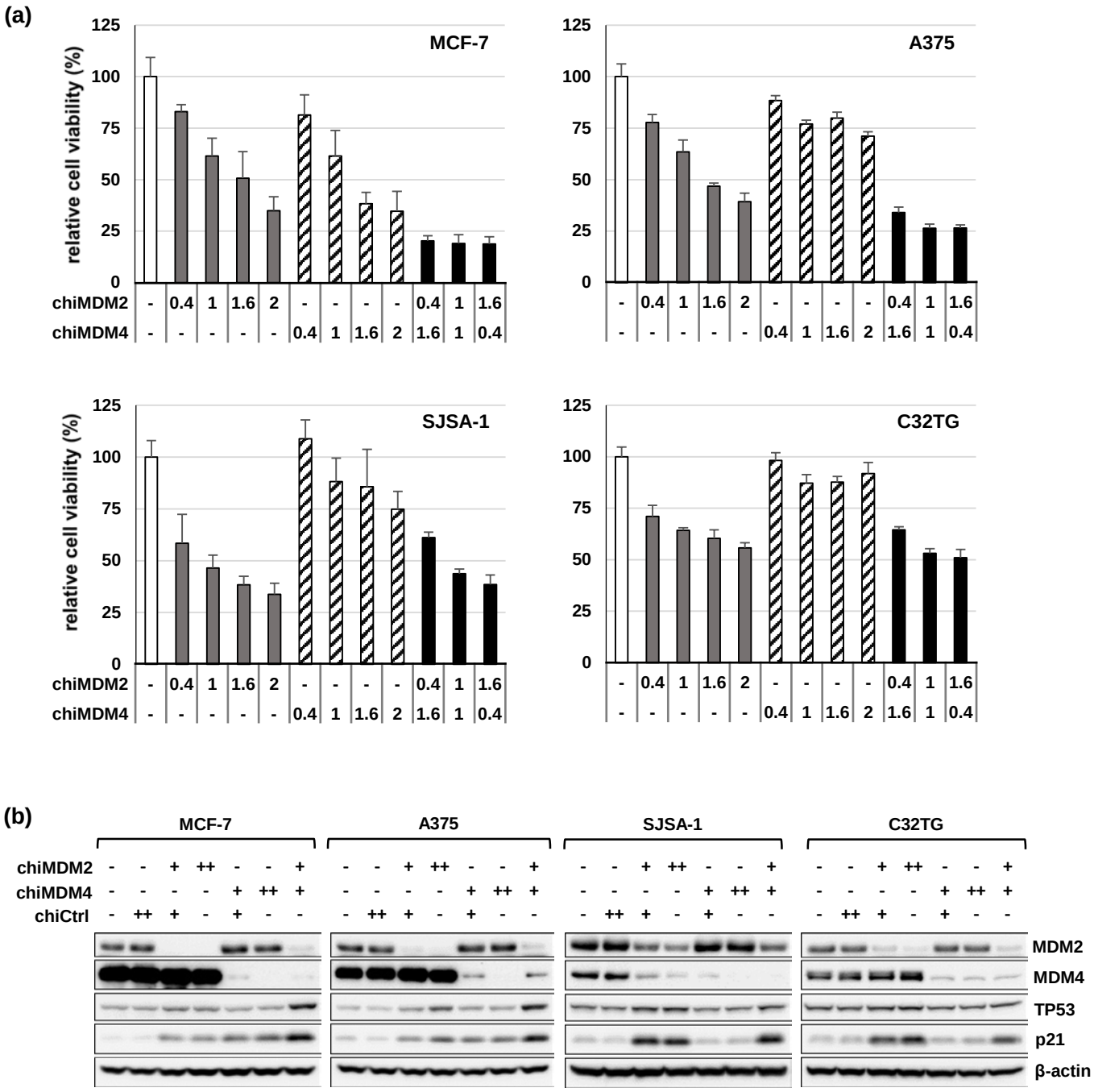
(a)
MCF-7
A375
SJSA-1
C32TG
relative cell viability (%)
125
100
75
50
25
0
chiMDM2 - 0.4 1 1.6 2 - - - - 0.4 1 1.6
chiMDM4 - - - - - 0.4 1 1.6 2 1.6 1 0.4
(b)
MCF-7
A375
SJSA-1
C32TG
chiMDM2 - - + ++ - - +
chiMDM4 - - - - + ++ +
chiCtrl - ++ + - + - -
MDM2
MDM4
TP53
p21
β-actin

Table 1. Combination index of chiMDM2 and chiMDM4 in MDM4 overexpressed cancer cell lines

chiMDM2 (nM)	chiMDM4 (nM)	Combination index						
		MCF-7	A375	SNU-1	HCT116	NUGC-4	LoVo	A549
0.4	1.6	0.57	0.20	0.36	0.17	0.26	0.55	0.55
1.0	1.0	0.51	0.28	0.39	0.43	0.39	0.45	0.65
1.6	0.4	0.47	0.20	0.56	0.44	0.63	0.31	0.72

CI>1.1, antagonistic effect; CI = 0.9–1.1, additive; CI<0.9, synergistic effects and the lower value means the stronger synergistic effect.

SUPPLEMENTAL MATERIALS

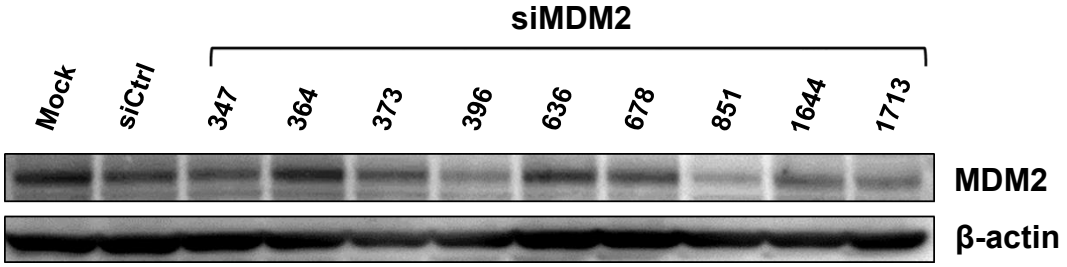

Supplementary Figure 1: Knockdown efficiency of siRNAs targeting *MDM2*. SJSA-1 cells were transfected with mock, control siRNA (siCtrl), and nine reported siMDM2s at 1 nM for 48 h and then examined for MDM2 expression by immunoblotting.

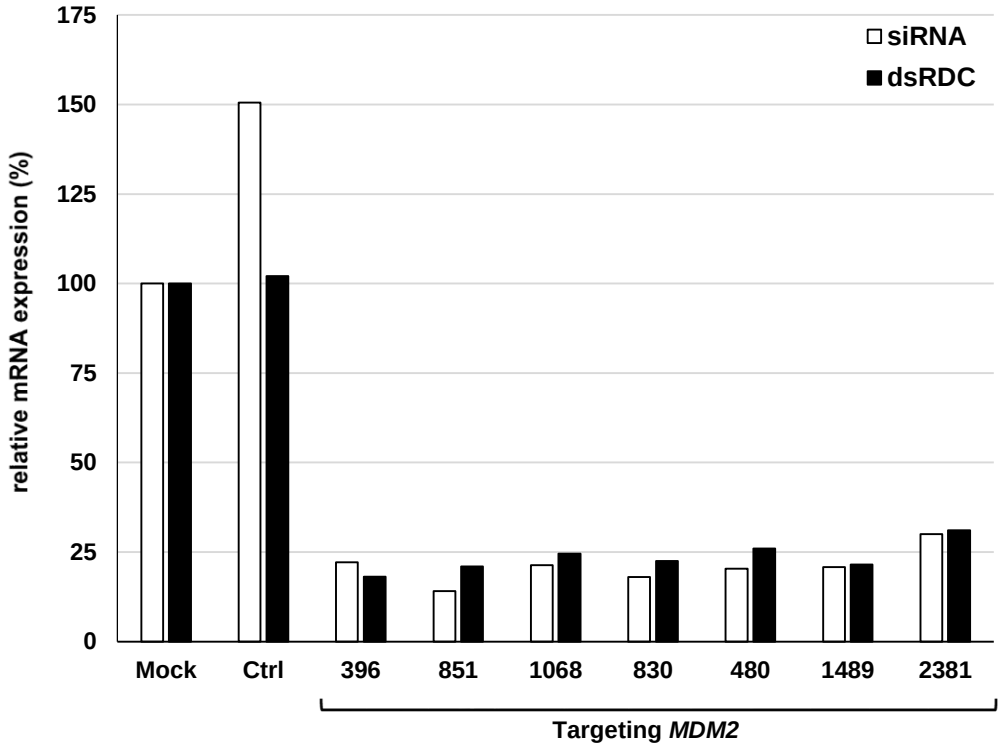

Supplementary Figure 2: Knockdown efficiency of siRNAs targeting *MDM2* and their dsRDC forms. SJSA-1 cells were transfected with mock, control (Ctrl) siRNA, seven siMDM2s, and their dsRDC forms at 1 nM for 48 h and then examined for *MDM2* mRNA expression by qRT-PCR. All experiments were performed in duplicate.

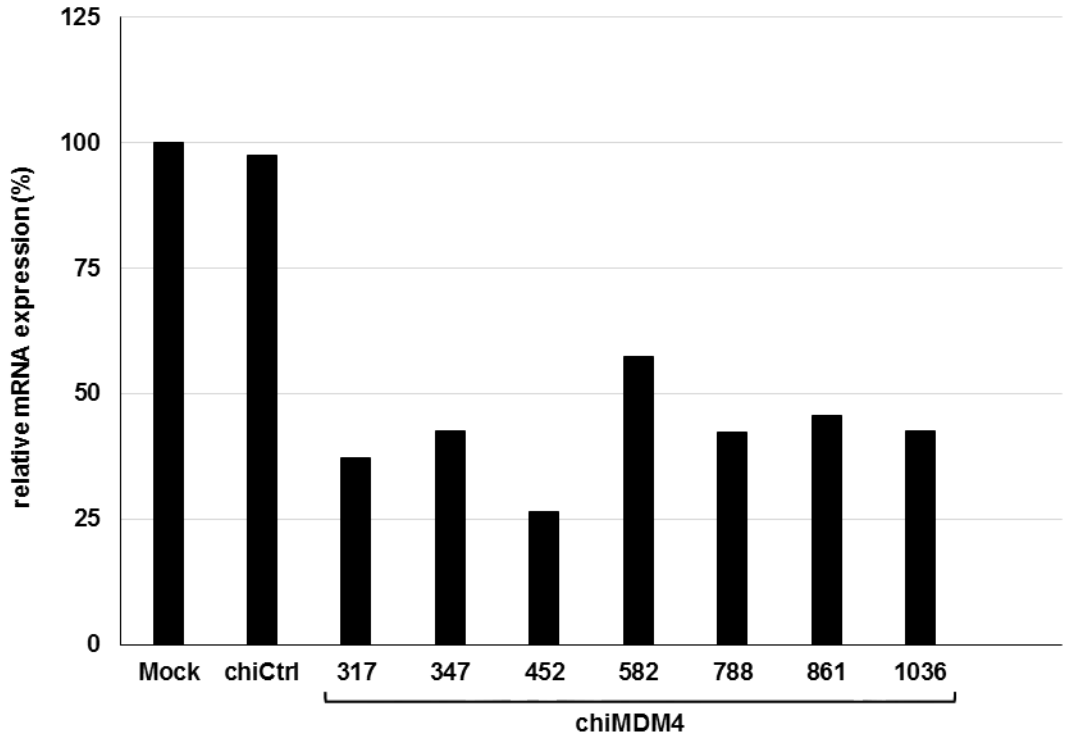

Supplementary Figure 3: Knockdown efficiency of dsRDC-modified siRNAs targeting *MDM4*. MCF-7 cells were transfected with mock, control dsRDC (chiCtrl), and seven dsRDCs targeting *MDM4* (chiMDM4) at 1 nM for 48 h and then examined for *MDM4* mRNA expression by qRT-PCR. All experiments were performed in duplicate.

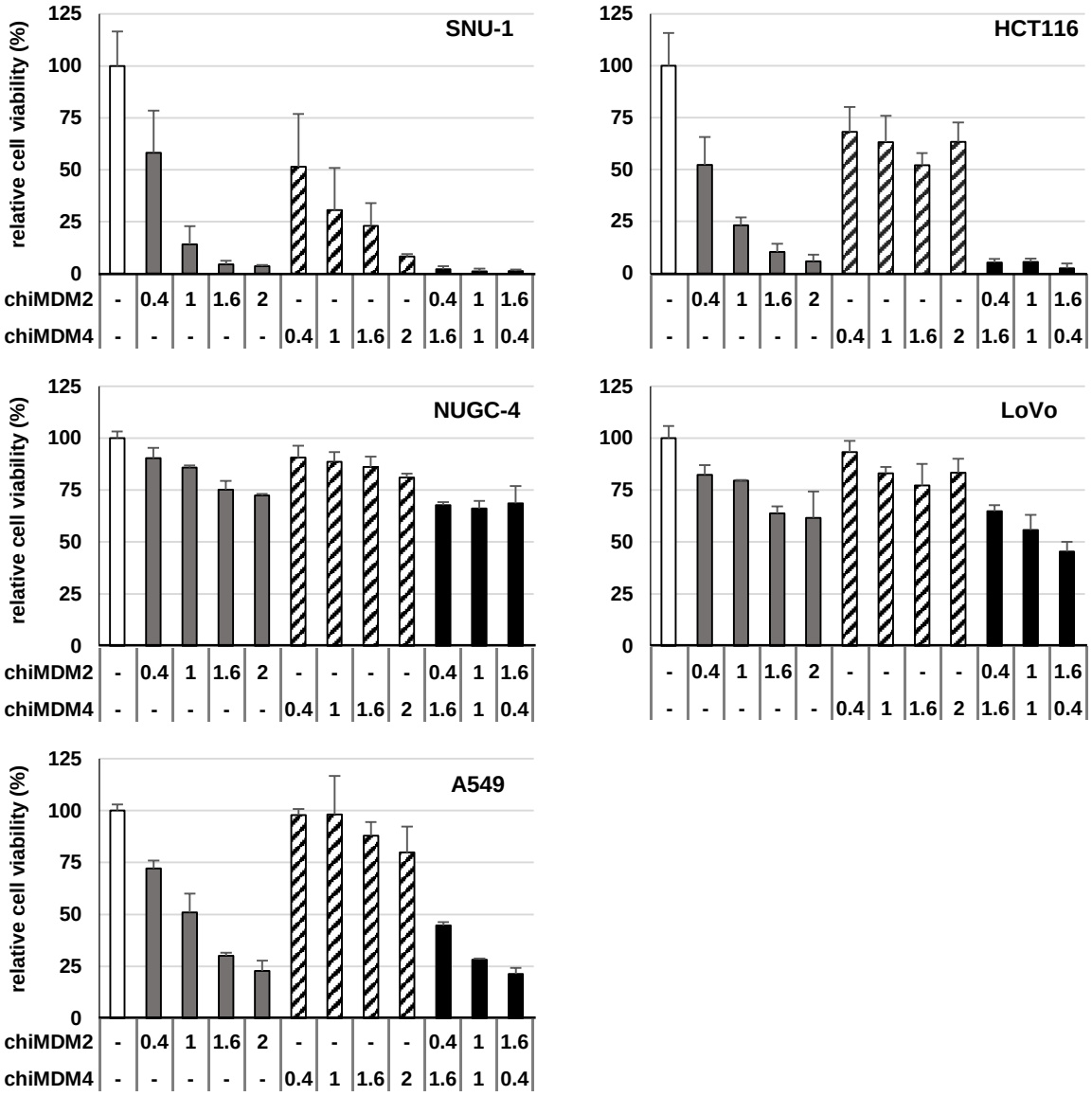

Supplementary Figure 4: Evaluation of combined knockdown of *MDM2* and *MDM4* on the growth of wt *TP53* cell lines with high MDM4 expression. Effects of individual and simultaneous knockdown of *MDM2* and *MDM4* on growth were examined in five wt *TP53* cell lines with high MDM4 expression. Cells were transfected with *MDM4* dsRDC (chiMDM4-452) alone, *MDM2* dsRDC (chiMDM2-1489) alone, or both. The total amount of dsRDC was adjusted to 2 nM by adding control dsRDC (chiCtrl). Cell viability was

determined 5 days after transfection using the WST-8 assay. The number of viable chiCtrl (2 nM) transfected cells was defined as 100% (mean ± SD; n = 3).

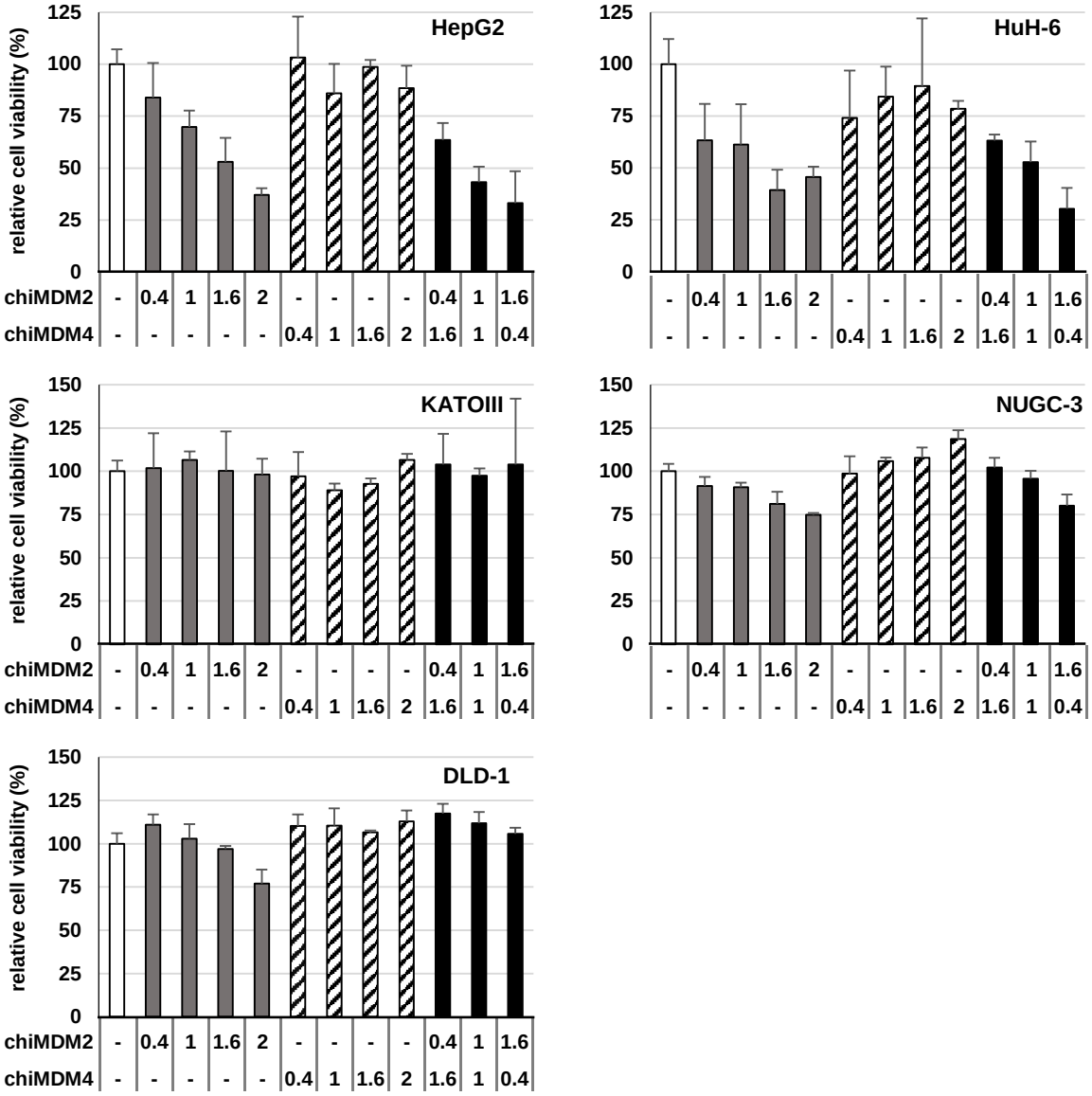

Supplementary Figure 5: Evaluation of combined knockdown of *MDM2* and *MDM4* on the growth of wt *TP53* cells with low MDM4 expression and mt *TP53* cells. Effects of individual and simultaneous knockdown of *MDM2* and *MDM4* on the cell growth were examined in wt *TP53* cells with low MDM4 expression (HepG2 and HuH-6) and mt *TP53* cells (KATOIII, NUGC-3, and DLD-1). Cells were transfected with *MDM4* dsRDC (chiMDM4-452) alone, *MDM2* dsRDC (chiMDM2-1489) alone, or both. The total amount of dsRDCs was adjusted to 2 nM by adding control dsRDC (chiCtrl). Cell viability was

determined 5 days after transfection using the WST-8 assay. The number of viable chiCtrl (2 nM) transfected cells was defined as 100% (mean ± SD; n = 3).

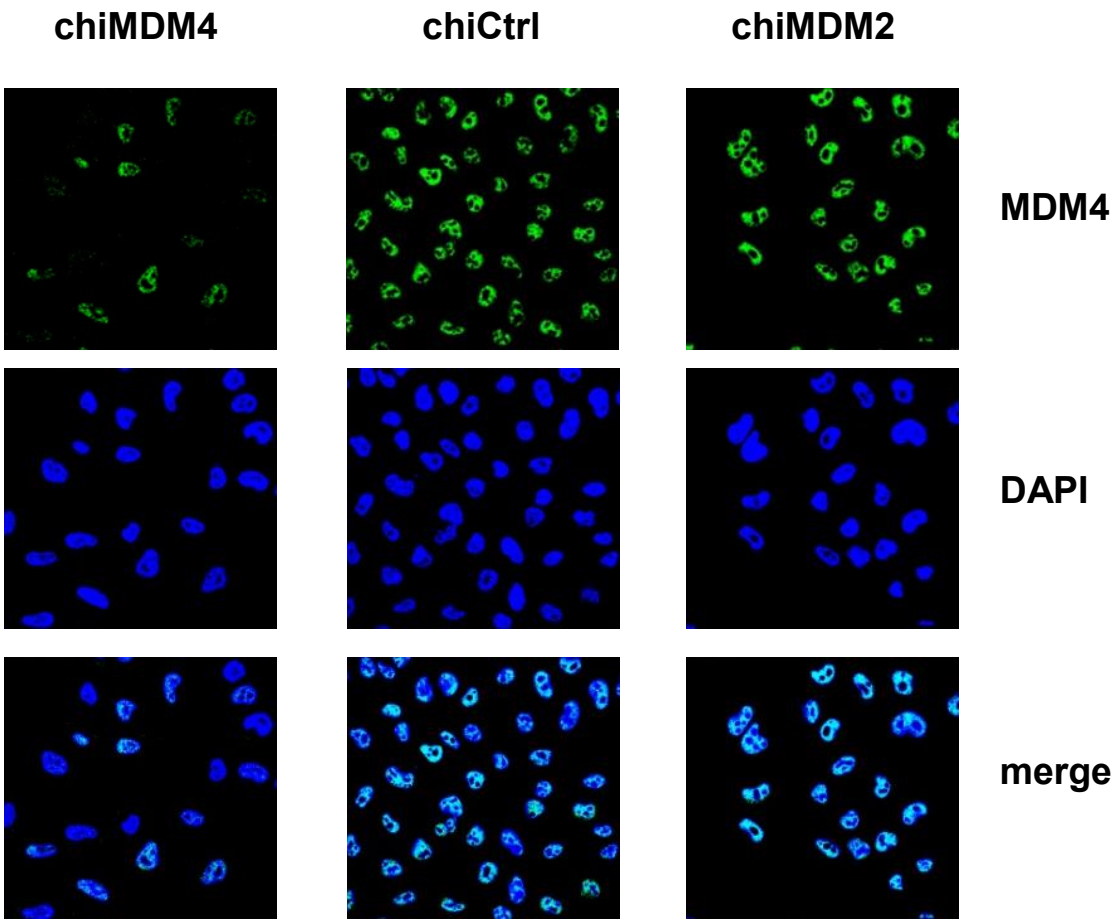

Supplementary Figure 6: Subcellular localization of MDM4 after *MDM2* knockdown. A375 cells were transfected with control dsRDC (chiCtrl), *MDM2* dsRDC (chiMDM2), or *MDM4* dsRDC (chiMDM4) at 1 nM for 24 h. Then, the localization of MDM4 was examined by immunofluorescence. Cellular nuclei were identified by DAPI staining.

Supplementary Table 1: Sequence of siRNAs

siRNAs	Nucleotide position	Passenger strand (5'→3')	Guide strand (5'→3')	References
siMDM2-347	347-369	CCACCUCACAGAUUCCAGCUU	GCUGGAAUCUGUGAGGUGGUU	Linares LK et al.
siMDM2-364	364-386	GCUUCGGAACAAGAGACCCUG	GGGUCUCUUGUUCCGAAGCUG	Yin JQ et al.
siMDM2-373	373-395	CAAGAGACCCUGGUUAGACCA	GUCUAACCAGGGUCUCUUGUU	Linares LK et al.
siMDM2-396	396-418	GCCAUUGCUUUUGAAGUUAUU	UAACUUCAAAAGCAAUGGCUU	Jin Y et al.
siMDM2-636	636-658	UCAGCAGGAAUCAUCGGACUC	GUCCGAUGAUUCCUGCUGAUU	Carrol VA et al.
siMDM2-678	678-700	CAGGUGUCACCUUGAAGGUGG	ACCUUCAAGGUGACACCUGUU	Toh WH et al.
siMDM2-851	851-873	GCCACAAAUCUGAUAGUAUUU	AUACUAUCAGAUUUGUGGCGU	Warburton HE et al.
siMDM2-1644	1644-1666	UGGUUGCAUUGUCCAUGGCAA	GCCAUGGACAAUGCAACCAUU	Kurki S et al.
siMDM2-1713	1713-1735	AAGGAAUAAGCCCUGCCCAGU	UGGGCAGGGCUUAUUCCUUUU	Uchida C et al.
siMDM2-480	480-502	GUAUAUUAUGACUAAACGAUU	UCGUUUAGUCAUAAUAUACUG	
siMDM2-643	643-665	GAAUCAUCGGACUCAGGUACA	UACCUGAGUCCGAUGAUUCCU	
siMDM2-691	691-713	GAAGGUGGGAGUGAUCAAAAG	UUUGAUCACUCCCACCUUCAA	
siMDM2-830	830-852	CUGGUGAACGACAAAGAAAAC	UUUCUUUGUCGUUCACCAGAU	
siMDM2-1068	1068-1090	CUCAGAAGAUUAUAGCCUUAG	AAGGCUAUAAUCUUCUGAGUC	
siMDM2-1274	1274-1296	CCCUUCGUGAGAAUUGGCUUC	AGCCAAUUCUCACGAAGGGCC	
siMDM2-1275	1275-1297	CCUUCGUGAGAAUUGGCUUCC	AAGCCAAUUCUCACGAAGGGC	
siMDM2-1489	1489-1511	CAGCCAUCAACUUCUAGUAGC	UACUAGAAGUUGAUGGCUGAG	
siMDM2-1625	1625-1647	GUCAAGGUCGACCUAAAAAUG	UUUUUAGGUCGACCUUGACAA	
siMDM2-2370	2370-2392	GGCCUAAAUGUCACUUAGUAC	ACUAAGUGACAUUUAGGCCGG	
siMDM2-2381	2381-3003	CACUUAGUACCUUUGAUAUAA	AUAUCAAAGGUACUAAGUGAC	
siMDM2-3412	3412-3434	CCACCAUUUACCCGUAAGACA	UCUUACGGGUAAAUGGUGGCU	
siMDM2-5187	5187-5209	CUCCAAAGGUAAAAGUACUAA	AGUACUUUUACCUUUGGAGGU	
siMDM2-6068	6068-6090	GGUUCUUUAUAGUACACGUGU	ACGUGUACUAUAAAGAACCUA	
siMDM2-6281	6281-6303	GCAGUUGGGAGCCUCCAAUGA	AUUGGAGGCUCCCAACUGCUU	
siMDM2-6393	6393-6415	GUGAUCGUGAAUGGUCUAUAA	AUAGACCAUUCACGAUCACUU	
siMDM2-7414	7414-7436	GUACUCAAAUAUUUAACGUUA	ACGUUAAAUAUUUGAGUACAG	
siMDM4-317	317-339	GGUCAUGCACUAUUUAGGUCA	ACCUAAAUAGUGCAUGACCUC	
siMDM4-347	347-369	GGUGAAGCAACUUUAUGAUCA	AUCAUAAAGUUGCUUCACCAU	
siMDM4-452	452-474	CCCUCUCUAUGAUAUGCUAAG	UAGCAUAUCAUAGAGAGGGCU	
siMDM4-525	525-547	GCUCUCGCACAGGAUCACAGU	UGUGAUCCUGUGCGAGAGCGA	
siMDM4-582	582-604	GCAGAGGAAAGUUCCACUUCC	AAGUGGAACUUUCCUCUGCAC	
siMDM4-788	788-810	CAACUAUACACCUAGAAGUAA	ACUUCUAGGUGUAUAGUUGCU	
siMDM4-861	861-883	GAUACUACAGAUGACUUGUGG	ACAAGUCAUCUGUAGUAUCUG	
siMDM4-1036	1036-1058	GUGAUGAUACCGAUGUAGAGG	UCUACAUCGGUAUCAUCACUU	
siMDM4-1492	1492-1514	GACCACGAGACGGGAACAUUA	AUGUUCCCGUCUCGUGGUCUU	
siMDM4-2263	2263-2285	GAGACUAUAGACUAGCAUAAC	UAUGCUAGUCUAUAGUCUCAG	
siControl		GUACCGCACGUCAUUCGUAUC	UACGAAUGACGUGCGGUACGU	
siControl-R		CCGUACUAGCCAUUAUGCGUC	CGCAUAAUGGCUAGUACGGGU	

Supplementary References

1. Linares LK et al. HdmX stimulates Hdm2-mediated ubiquitination and degradation of p53. Proc Natl Acad Sci USA. 2003; 100: 12009-14
2. Yin JQ et al. siRNA agents inhibit oncogene expression and attenuate human tumor cell growth. J Exp Ther Oncol. 2003; 3: 194-204
3. Jin Y et al. MDM2 promotes p21waf1/cip1 proteasomal turnover independently of ubiquitylation. EMBO J. 2003; 22: 6365-77
4. Carrol VA et al. Regulation of angiogenic factors by HDM2 in renal cell carcinoma. Cancer Res. 2008; 68: 545-52
5. Toh WH et al. Relief of p53-mediated telomerase suppression by p73. J Biol Chem. 2005; 280: 17329-38
6. Warburton HE et al. p53 regulation and function in renal cell carcinoma. Cancer Res. 2005; 65: 6498-503
7. Kurki S et al. Nucleolar protein NPM interacts with HDM2 and protects tumor suppressor protein p53 from HDM2-mediated degradation. Cancer Cell. 2004; 5: 465-75
8. Uchida C et al. Enhanced Mdm2 activity inhibits pRB function via ubiquitin-dependent degradation. EMBO J. 2005; 24: 160-169